AD-A070 945 MASSACHUSETTS INST OF TECH CAMBRIDGE CENTER FOR SPAC--ETC F/G 3/2
ANALYSIS OF SOLAR WIND DATA FROM THE SOLRAD 11A AND 11B SPACECR--ETC(U)
FEB 79 A J LAZARUS F19628-75-C-0131

UNCLASSIFIED AFGL-TR-79-0056 NL

1 OF

AD
A070945

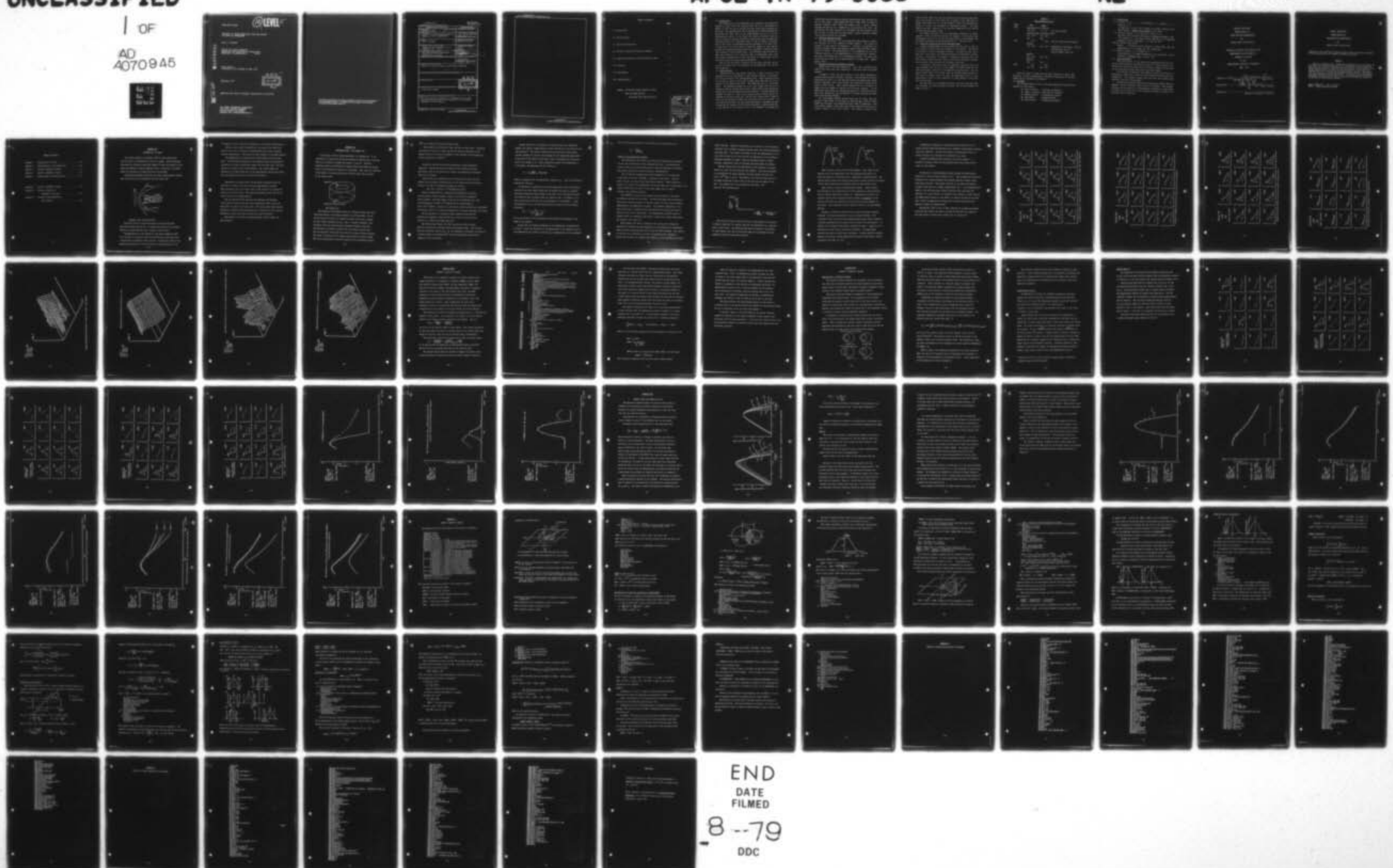

END
DATE
FILMED
8 --79
DDC

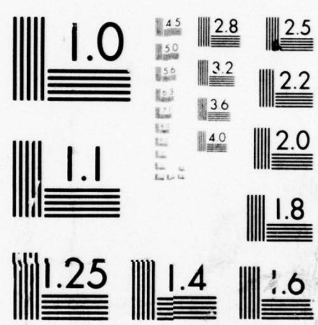

MICROCOPY RESOLUTION TEST CHART
NATIONAL BUREAU OF STANDARDS-1963-A

(10) LEVEL II

AFGL-TR-79-0056

ANALYSIS OF SOLAR WIND DATA FROM THE SOLRAD 11A AND 11B SPACECRAFT

Alan J. Lazarus

Center for Space Research
Massachusetts Institute of Technology
Cambridge, Massachusetts 02139

Final Report
1 February 1975 through 31 May 1978

February 1979

Approved for public release; distribution unlimited.

AIR FORCE GEOPHYSICS LABORATORY
AIR FORCE SYSTEMS COMMAND
UNITED STATES AIR FORCE
HANSCOM AFB, MASSACHUSETTS01731

Unclassified

MIL-STD-847A
31 January 1973

SECURITY CLASSIFICATION OF THIS PAGE (When Data Entered)

19 REPORT DOCUMENTATION PAGE		READ INSTRUCTIONS BEFORE COMPLETING FORM
1. REPORT NUMBER 18 AFGL-TR-79-0056	2. GOVT ACCESSION NO.	3. RECIPIENT'S CATALOG NUMBER
4. TITLE (and Subtitle) 6 ANALYSIS OF SOLAR WIND DATA FROM THE SOLRAD 11A and 11B SPACECRAFT		5. TYPE OF REPORT & PERIOD COVERED 1 Feb 1975-31 May 1978 Final Report
		6. PERFORMING ORG. REPORT NUMBER
7. AUTHOR(s) 10 ALAN J. LAZARUS		8. CONTRACT OR GRANT NUMBER(s) 15 F19628-75-C-0131
9. PERFORMING ORGANIZATION NAME AND ADDRESS CENTER FOR SPACE RESEARCH, M.I.T., CAMBRIDGE, MA 02139		10. PROGRAM ELEMENT, PROJECT, TASK AREA & WORK UNIT NUMBERS 62101F 17 G1 16 2311G1AD
11. CONTROLLING OFFICE NAME AND ADDRESS AIR FORCE GEOPHYSICS LABORATORY Hanscom AFB, Ma 01731 Monitor/G. K. Yates/PHG		12. REPORT DATE 11 ~~February 1979~~
		13. NUMBER OF PAGES 89 12 89p.
14. MONITORING AGENCY NAME & ADDRESS(if different from Controlling Office)		15. SECURITY CLASS. (of this report) Unclassified
		15a. DECLASSIFICATION/DOWNGRADING SCHEDULE N/A

16. DISTRIBUTION STATEMENT (of this Report)

Approved for public release; distribution unlimited.

9 Final rept. 1 Feb 75-31 May 78

17. DISTRIBUTION STATEMENT (of the abstract entered in Block 20, if different from Report)

DDC
RECEIVED
JUL 10 1979
B

18. SUPPLEMENTARY NOTES

19. KEY WORDS (Continue on reverse side if necessary and identify by block number)

Solar Wind, SOLRAD

20. ABSTRACT (Continue on reverse side if necessary and identify by block number)

The data reduction, analysis, and interpretation of solar wind data obtained from the MIT experiment on the SOLRAD spacecraft are described.

DD FORM 1 JAN 73 1473 EDITION OF 1 NOV 65 IS OBSOLETE

UNCLASSIFIED
SECURITY CLASSIFICATION OF THIS PAGE (When Data Entered)

403 837

JOB

TABLE OF CONTENTS

1.0 Introduction

The primary goal of the processing, data reduction, and scientific analysis of solar wind data obtained from the M.I.T. experiments on SOLRAD 11A and 11B, was to provide real-time solar wind parameters to DOD users. The secondary goal was an extraction of detailed parameters describing the solar wind in the magnetosheath as well as in the interplanetary medium. It was hoped that special attention could be given to periods of special scientific interest and that the high time resolution mode of the instrument could be used to advance our knowledge of the nature of magnetohydrodynamic processes in the solar wind. In particular, the first month of operation seemed to hold special promise for interesting physics since the two SOLRAD 11 spacecraft were close together as they orbited Earth. An additional hope was that the high time resolution data could be used in combination with radio scintillation measurements to find the source of fluctuations in the wind which caused the scintillation phenomenon.

Most of the anticipated outcomes were partially achieved; but as will be discussed below, the potential of the experiment could not be fully exploited.

2.0 Real-time data

Preparations were made before launch for a rapid analysis of the real-time data and calculation of the velocity, density, temperature, and flow direction of the interplanetary wind. These parameters were to be sent in close to real time to NOAA where they were to form a portion of the SELDADS data base. The effort got off to a very slow start: the programs prepared by M.I.T. were ready; but the cut in funding at NRL had reduced their staff to such a point that operational matters had to take precedence over data analysis. Although SOLRAD was launched on March 14, 1976, there remained several months before the problems at NRL were cleared up. The data were finally sent to NOAA in 1977, and the problems at NOAA were not solved until late in 1977. In the intervening period, the data system had begun to scramble our data by rotating the sequence of bits which represented a complete spectrum. A good portion of our effort at M.I.T. was expended in decoding the rotated data and developing an analysis system which could retrieve the data in most cases. That program was sent to NOAA where it began to function normally. NOAA itself was plagued with a severe funding shortage and much to do. SOLRAD had a low priority late 1977. The interaction with NOAA required our clarifying the data sequence from NRL for them. At long last the whole system worked. Meanwhile, SOLRAD 11A had failed totally in an eclipse.

3.0 Detailed analysis of data

The full description of this process and the scientific results are contained in a S.B. thesis by Michael Herrera. The thesis is included in this report as Appendix A. Briefly, he describes the detailed analysis process and presents results from different regions around the earth. The determination of the parameters of the distribution function in the magnetosheath is of considerable interest. The solar wind interaction is of considerable interest. The solar wind interaction with Venus can be characterized in a similar way. (Shefer _et al._, 1979).

4.0 Periods of specified scientific interest

SOLRAD solar wind data analyzed at M.I.T were available more rapidly than those from other spacecraft. They were used for diverse purposes.

In August of 1976, the third section of the Skylab workshop on coronal holes was held in Boulder, Colorado. Good correlation had been established by the M.I.T. and American Science and Engineering groups between high-speed solar wind streams and equatorial coronal holes viewed in soft x-rays. Solar minimum appeared to be in progress as judged from the absence of optical and UV coronal features. It was SOLRAD data which showed the continuing presence of a high speed stream and, hence, showed that the relationship to coronal processes was more subtle than had been assumed.

The relationship between coronal holes and the solar wind was studied in more detail in the paper by (Nolte _et al._, 1977) in which SOLRAD and IMP solar wind observations were used in comparison with x-ray coronal images to show that high speed streams were very much in evidence despite a very quiet corona. The authors concluded that either coronal holes were not the sources of all recurring high-speed solar wind streams or that there was a change in the appearance of regions which gave rise to the open magnetic field line configuration thought to promote the emergence of high-speed streams. The same observations were reported at the American Geophysical Union Spring Meeting (Sullivan et al., 1977).

The SOLRAD data were also of considerable assistance in establishing a cross calibration between the Voyager 1 and 2 solar wind instruments, which had a ten per cent uncertainty in calibration, and the SOLRAD instrument, which was calibrated to $\sim$ three per cent.

5.0 High-time resolution and close spacecraft data

A great disappointment in the progress of this work is that we were unable to exploit these two features of the mission. The reason is a mixture of lack of personnel and data. It should be clear that a good deal of our effort was expended developing an algorithm to correct the data. Furthermore, the amount of high-time resolution data was quite limited since we did not wish to (nor were we allowed) to preempt time from other experimenters for our special data mode.

In practice, that meant that the high-time resolution data are only available near the end of the SOLRAD 11B lifetime when all the other operational problems of the spacecraft settled down. We certainly cannot object--it is clear that the limited funds available at NRL forced an heroic effort to keep the spacecraft alive at all. Nevertheless, there is still potential for good physics in the data that are available.

The data from the two SOLRAD spacecraft taken when they were near to one another are also potentially valuable, but far from complete as shown in Table 1.

Table 1

Data Received at M.I.T.

Year	Day	Pass	
1976	Experiments not turned on		
	84 - 89	7 - 11	S/C close together
	missing (tapes available at NRL)		
	177 - 274	82 - 160	
	275 -	161 -	
1977	- 05	- 238	11B S/C timing circuit failure
	missing		
	97 - 116	312 - 327	Experiment on 11A failed - Day 116
			11B Data bad, Day 133
			11A S/C failed, June 1977
	missing		
	236 - 255	424 - 439	
	missing		
	296 -	472	
1978	- 20	- 543	
	30 - 59	552 - 575	

Only four days of close data had been received by early 1979, therefore, we had no opportunity to explore the potential of the data though they are available in principle.

6.0 Personnel

The following people at M.I.T. have been associated with the work described in this report:

Dr. Alan J. Lazarus - Principal Investigator
Dr. James D. Sullivan - Post-doctoral Scientist
Mr. Michael Herrera - Undergraduate Student
Ms. Ruth Shefer - Graduate Student
Mr. Jules Mollere - Undergraduate Student

7.0 Bibliography

J. T. Nolte; Davis, J. M., Gerrasimenko, M., Lazarus, A. J., Sullivan, J. D.

A Comparison of Solar Wind Streams and Coronal Structure Near Solar Minimum. Geophys. Res. Letters 4, 291 (1977).

J. D. Sullivan, Lazarus, A. J., Nolte, J.T.,Davis, J. M.

The Solar Wind and Coronal Structure in September/November, 1976, talk presented at the Annual Spring Meeting of the American Geophysical Union, Washington, D. C., May 30, 1977.

Herrera, Michael Dardo Steven

SOLRAD: Preliminary Plasma Results in (the) Solar Wind and Magnetosheath, S. B. Thesis, May 1977, unpublished.

R. E. Shefer, Lazarus, A. J., Bridge, H. S.

A Re-examination of Plasma Measurements from the Mariner 5 Venus Encounter, J. Geophys. Res. in press, 1979.

8.0 Acknowledgements

The work described in this report was accomplished only with the patient understanding of the contract monitor, Dr. Kenneth Yates, who accepted the limitations imposed by the difficult funding restrictions, and who persevered through late reports and other delays.

The Principal Investigator also wishes to thank the Air Force for funding this analysis at a time when other sources of funds had all but disappeared. The insights gained from this work have already made important scientific contributions.

The Tektronix computer system was purchased with support from the National Science Foundation under Grant ATM 76-82108. Any opinion, findings, and conclusions or recommendations expressed in this report are those of the author and do not necessarily reflect the views of the National Science Foundation.

SOLRAD: PRELIMINARY

PLASMA RESULTS IN

SOLAR WIND AND MAGNETOSHEATH

by

Michael Dardo Steven Herrera

SUBMITTED IN PARTIAL FULFILLMENT OF THE

REQUIREMENTS FOR THE DEGREE OF

BACHELOR OF SCIENCE

at the

MASSACHUSETTS INSTITUTE OF TECHNOLOGY

May, 1977

Signature of Author......Michael Dardo Steven Herrera......
Department of Physics, May 27, 1977

Certified by..............Alan J. Lazarus..............
Alan J. Lazarus

Accepted by..
Chairman of Departmental Committee

SOLRAD: PRELIMINARY

PLASMA RESULTS IN

SOLAR WIND AND MAGNETOSHEATH

by

Michael Dardo Steven Herrera

Submitted to the Department of Physics on May 27,1977 in partial fulfillment of the requirements for the Degree of Bachelor of Science

ABSTRACT

This is a research report on analysis of Experiment 15 on the Solrad 11A and Solrad 11B satellites being done at the MIT Center for Space Research. This experiment involves plasma detectors that measure current within differential energy channels for positive ions and electrons. The satellites transmit data from the solar wind and magnetospheric regions. This report will concentrate on a preliminary analysis of the positive ion distribution functions determined from the Solrad data. A graphics display minicomputer and separate Fortran programs serve to determine characteristic parameters of and plot the distribution functions.

THESIS SUPERVISOR: Alan J. Lazarus
TITLE: Senior Research Scientist

TABLE OF CONTENTS

CHAPTER ONE

INTRODUCTION TO SOLRAD

Our earth's magnetic environment offers an ideal opportunity for the study of a collisionless shock in a plasma. With a long mean free path and relatively long Debye length, of about ten meters, of the plama surrounding our earth's magnetic field, a satellite is an ideal probe for surveying the characteristics of this plasma.

The following diagram illustrates the basic magnetospheric regions about the earth and its interaction with the solar wind.

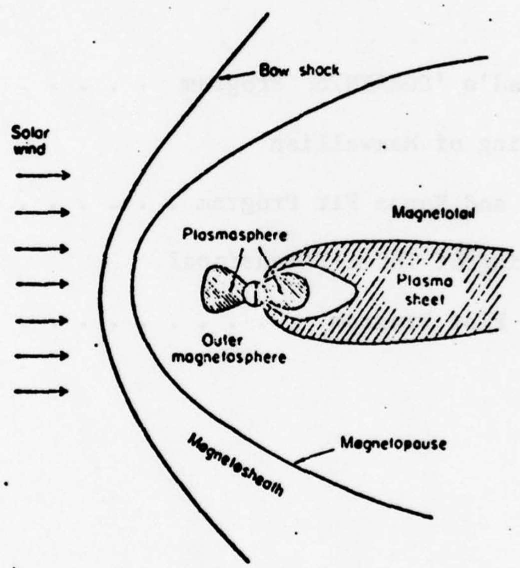

(diagram taken from Vasyliunas)

The solar wind is a stream consisting of protons and alpha particles flowing from the sun. It reaches the earth with an average velocity of around 400 km/s with a density of about 10/cc.

The magnetopause is the boundary of the earth's magnetic field. It is located at a distance where the pressure due to the solar wind is balanced by the magnetic field pressure. The density inside of the magnetopause boundary is much less than that found outside of it as the magnetic field is generally impermeable to the plasma flowing past it.

Since the solar wind is hypersonic at the earth (with Alvén wave speed on the order of 50 km/s), a detached shock wave exists upstream from the magnetopause. This marks the outer boundary of the magnetosheath.

The magnetosheath is qualitatively very different from the solar wind. A collisionless mechanism at the bowshock raises its temperature and density to values considerably higher than the solar wind. The bulk velocity is reduced and its angle shifted. Also, there exists the phenomenon of a high energy tail in the magnetosheath spectra that differ from the Maxwellian nature of the solar wind spectra.

Experiment #15 aboard Solrad 11A and Solrad 11B detects ions and electrons of plasma in the solar wind and magnetospheric regions. These satellites orbit in a plane close to the ecliptic at a geocentric distance of 20 earth radii. They spend approximately equal time in the solar wind and in the magnetosphere.

The two satellites were launched simultaneously and remained close together initially but were later separated by 180° so that one spacecraft is always in the solar wind. This also enables more complete tracking by tracking sites in Blossom Point, Virginia and in the Arcetri Observatory, Italy, the latter of which has only one antenna.

This report is a record of ongoing research at MIT's Center for Space Research.

CHAPTER TWO

INSTRUMENTATION - THE FARADAY CUP

At the heart of MIT's plasma experiment is a Faraday cup. It is comprised of a modulated grid situated between an aperture and a collector plate in a cylindrical package that points to the sun. The grid modulation selects the differential energy window from which the average value of the distribution function is calculated. This value is a function of the amount of current striking the collector plate and the width of the energy window.

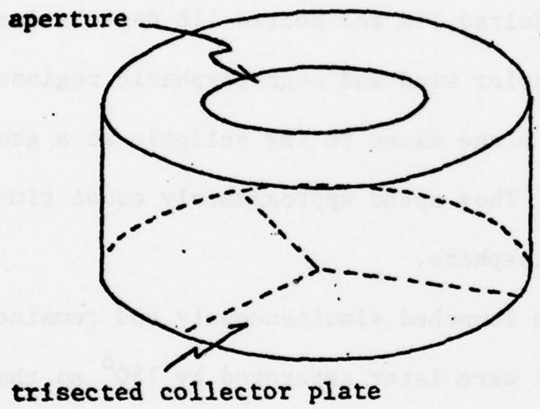

the faraday cup

The voltage on the modulated grid is a 500 Hertz square wave that alternates between two voltages referred to as VHI and VLOW. The DC current from the collector is caused by positive ions with an energy per unit charge associated with V_z, the z - velocity component, that is greater than the instantaneously impressed voltage on the grid. The difference in absolute current from the collector between that with the high grid voltage and that with the low grid voltage indicates the number of particles in the energy range defined by these voltages. This current difference is directly measured as an alternating current

180^{o} out of phase with the modulating voltage.

The collector is divided into three sections of equal area. Utilizing the ratios of currents in these sections, the angle of incidence of the plasma relative to the axis of symmetry of the cylinder of the Faraday cup can be calculated to within 2^{o}.

Circuitry controls the AC and DC components of grid modulation separately. 'Electrometers' are AC coupled to each collector section. Any problem with the DC photoelectric effect is sufficiently eliminated with the AC coupling.

Current data are transmitted from the spacecraft by means of data numbers that correspond logarithmically to the inverse of the current as follows (for DN the datanumber and CURR the current).

$$DN = 255. + \ln(6.94 \times 10^{-13}/CURR)/\ln(1.0367)$$

This is accomplished by a logarithmic Analog/Digital converter. In this manner currents through a range of four orders of magnitude can be encoded. Each data number is written as a hexidecimal pair with 00 corresponding to 6.806×10^{-9} amperes and FF corresponding to 6.94×10^{-13} amperes. Because the current/data number conversion is logarithmic the limiting error due to discrete datanumbers is constant throughout the range.

In our experiment 24 contiguous energy channels, detecting the positive ion component, range from 241 ev to 4279 ev for protons and from 482 ev to 8559 ev for alpha particles.

One large energy channel, the 30th, measures the total current from ions striking the collector within these energy limits. The currents from each individual sector of no. 30 are registered in channels 31,32,and 33. A second Faraday cup positioned 90^{o} from the sun measures the electron component of the solar wind.

Current density for a collection of particles each with individual charge q and overall number density n equals $nq\vec{v}$ when all particles have the same velocity $\vec{v}$. The current collected at the collector of the faraday cup must therefore be equal to the average value of $(nq\vec{v})\cdot A(\vec{v})\hat{n}$ where $A(\vec{v})$ is the area of the portion of the plate that is illuminated by the plasma and $\hat{n}$ is the normal to it. Thus, taking into account the transparency, τ, of the grids, the expression for the current is

$$I = \tau nq \iiint_{-\infty}^{\infty} v_z \; f(\vec{v})A(\vec{v})d\vec{v}$$

which is integrated over the appropriate limits for v_z. $f(\vec{v})$ is the velocity distribution function.

To determine an expression for $f(\vec{v})$ we assume that it can be considered constant within each energy window, and we consider the angle of incidence and plasma temperature small enough so that $A(\vec{v})$ can be considered constant (the aperture area is smaller than the collector area - in Chapter V the error resulting from making such an approximation is considered). Then the expression for f_n, the distribution function value in the nth channel is given by

$$f_n \propto \frac{I_n}{\tau nq \iiint v_z \, d\vec{v}}$$

for I_n the current in the nth channel and the limits corresponding to the range of the channel.

We see that the integral expression in the denominator is proportional to $(v2_n)^2 - (v1_n)^2$ and therefore to the energy width of the channel, ΔE_n. As I am considering only relative values for f_n, normalization is not considered and the following expression is used without the determination of k:

$$f_n = \frac{k\, I_n}{(q/m)\Delta E_n}$$

Plots of the Distribution Function

The Techtronics 4051 computer was then used to make plots of spectra for the data transferred from the original data tape. The abscissa was scaled to show v_z of protons with each tic mark corresponding to 100 km/s. The spectra could then be seen on linear or semilog plots.

The '15 Spectra' program inputs the datanumbers for 15 cycles from a tape file in the data cartridge. From each it calculates , from the above formula, the value of the distribution function. These values are placed in an array F(I,J) dimensioned as F(24,15) where the I corresponds to the channel number minus one and J to the index number that is used to reference each individual spectra.

The VIEWPORT function in the program allows the graph to be placed in different portions of the screen. The following pages show distribution functions in semi-log plotted for various regions: the solar wind, bowshock, magnetosheath, and magnetopause regions. The parabolic appearance of the solar wind plots is consistent with the Maxwellian function being known to provide a good fit for these cases. The magnetosheath examples cannot be closely fitted to a Maxwellian and Chapter V shows that a Kappa distribution may provide a very close fit.

These graphs, and others I compiled, seem to hold much information regarding the changing of plasma parameters in the bowshock and magnetopause regions and more investigations will be done of these crossings. One problem to overcome is the separation of proton and alpha-particle components. Another factor making the analysis more complex, is the existence of multiple shock crossings. Temporal fluctuations can be noticed in certain spectra resulting from a bowshock crossing occurring while the current measurements are being taken. How rapidly the change is from the magnetosheath to the solar wind portion of the curve can give an indication as to the shock's thickness dividedby its speed. From the intended analysis of shock velocity, significant values of thickness and speed might be obtained.

The dots placed below the distribution curve represent the lowest value of f_n that can be plotted for each channel. They each correspond to the datanumber FF which signifies that the original currents are 6.94×10^{-13} amps or below. The numbers on the top left hand corner of the pages containing 15 plots refer to the year and day number of the year. The numbers found in each graph are the hours. The axes have the following scale.

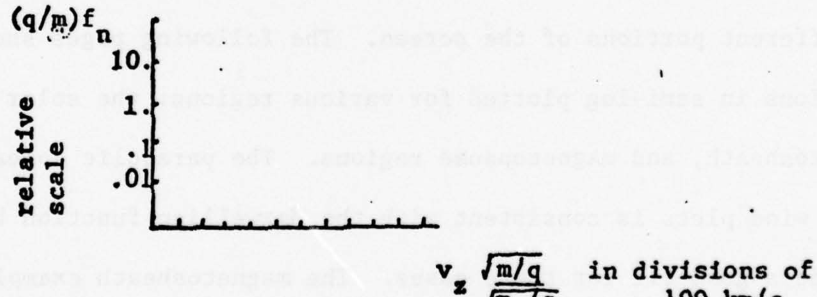

The proton and alpha particle spectra are superimposed on the graph. A computer summation of a typical case with two Maxwellians on a semi-log plot is shown below. The alpha-particle peak is located at an abscissa $\sqrt{2}$ times greater than that of the proton peak (as is expected for both components having the same bulk velocity).

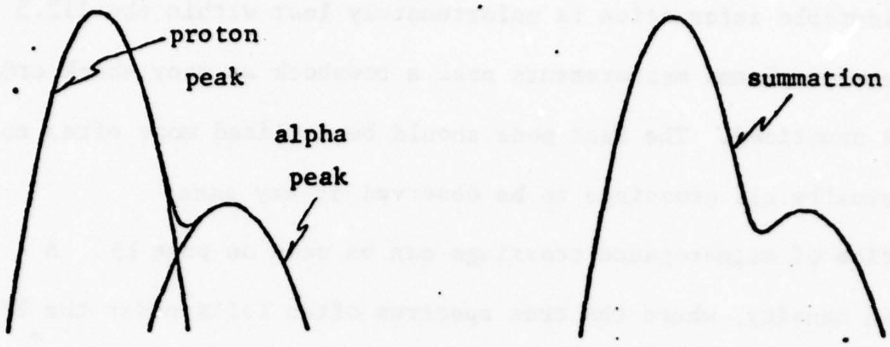

Page 10 shows a series of solar wind samples. Their shape is the expected sum of two Maxwellians, with the alpha-particle peak at $\sqrt{2}$ times the abscissa of the proton peak. Bulkspeed is around 600 km/s. The relative density (from the ordinate being qf/m) of alpha particles to protons ≈ 6% by number assuming both components have the same thermal speed.

Page 11 shows a series of magnetosheath samples. Thermal speeds are increased so that identification of each component is made difficult (this is further explained in chapter 5). Magnetosheath particles, as is observed here have a characteristically smaller z-component of bulk velocity (from both the reduction of bulk velocity and the geometry of the shock). The z-component of bulk velocity, bulkvz, is in this sample, 350 km/s.

On page 12 is found an excerpt from a series of multiple bowshock crossings. The solar wind speed is seen to be about 400 km/s. The 'turbulence' that is found in these magnetosheath spectra seem to indicate a certain superposition of particles with the solar wind distribution. An example of the temporal fluctuations, mentioned on page 7 , seems to be in the spectra at hour 2323 at the 300 km/s position. The high-energy particle fluctuation in 2325 seems intriguing. It might signify a periodic temporal fluctuation, between magnetosheath and solar wind states, having a period on the order of 1 sec.

Considerable information is unfortunately lost within the 112.5 seconds between plasma measurements near a bowshock as many shock crossings would pass unnoticed. The fast mode should be utilized more often to enable virtually all crossings to be observed in any pass.

A series of magnetopause crossings can be seen on page 13. A decrease in density, where the true spectrum often falls under the FF curve, is most evident.

Projections of three-dimensional graphs showing the distribution function vs. time are found on pages 14 to 17. This provides an informative perspective for viewing temporal (and possibly spacial) changes within each energy interval. The density variation in the solar wind spectra on page 14 may indicate a regular compressional wave. In the magnetosheath sample on the following page, regular variations also seem apparent. Although a bit more difficult to visualize, the 'plateau' on page 16 shows the magnetosheath spectra in the middle of a double crossing of the shock. Page 17 shows a magnetopause crossing where the peaks along the time dimension signify the magnetosheath.

Two parallel lines in the t-v plane indicate the minimum and maximum velocities that Solrad can detect, 215 km/s and 905 km/s. The range of the time domain is listed under 'Solrad 11A' or 'Solrad 11B'.

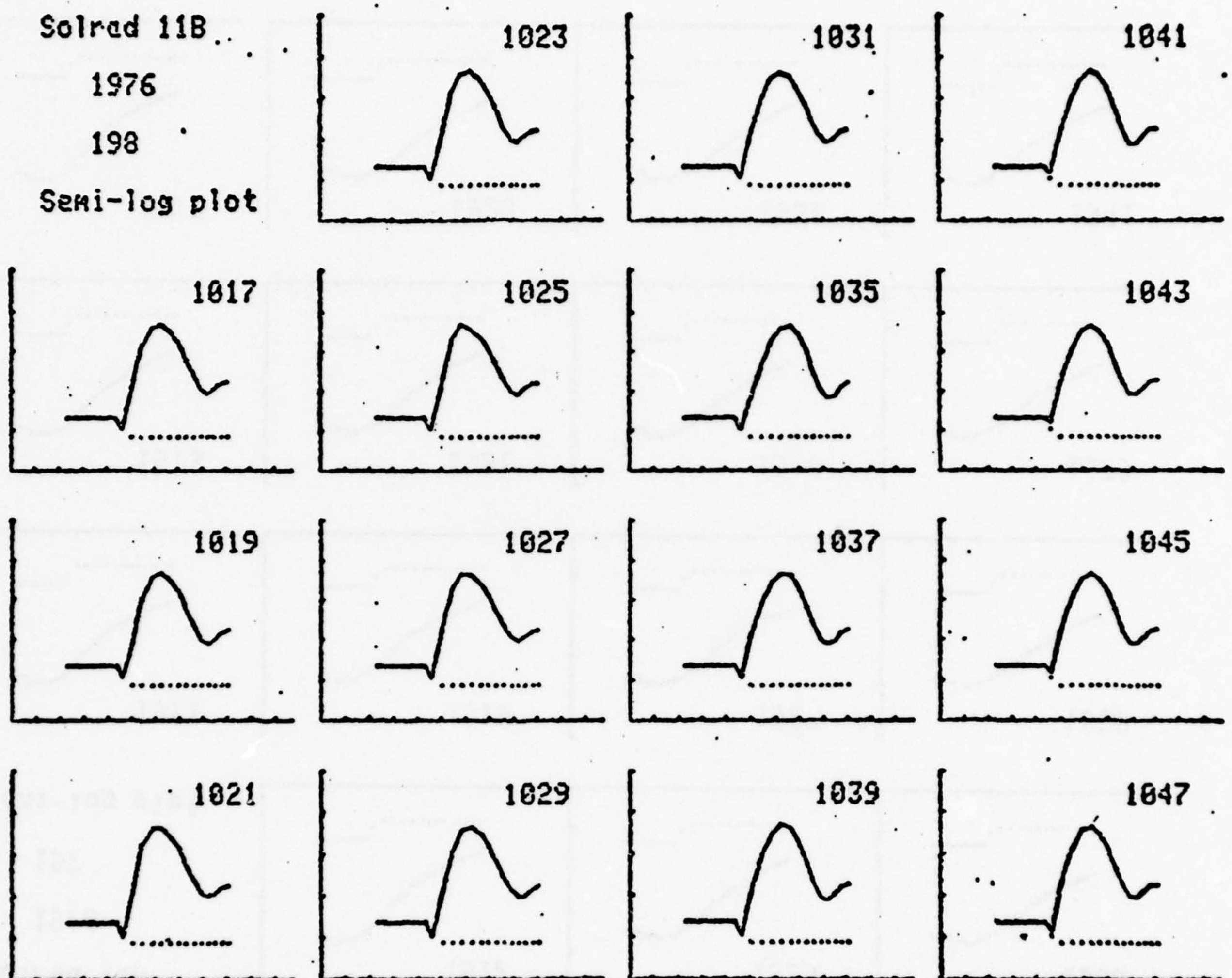

A typical example of a series of solar wind spectra not found near the bowshock.

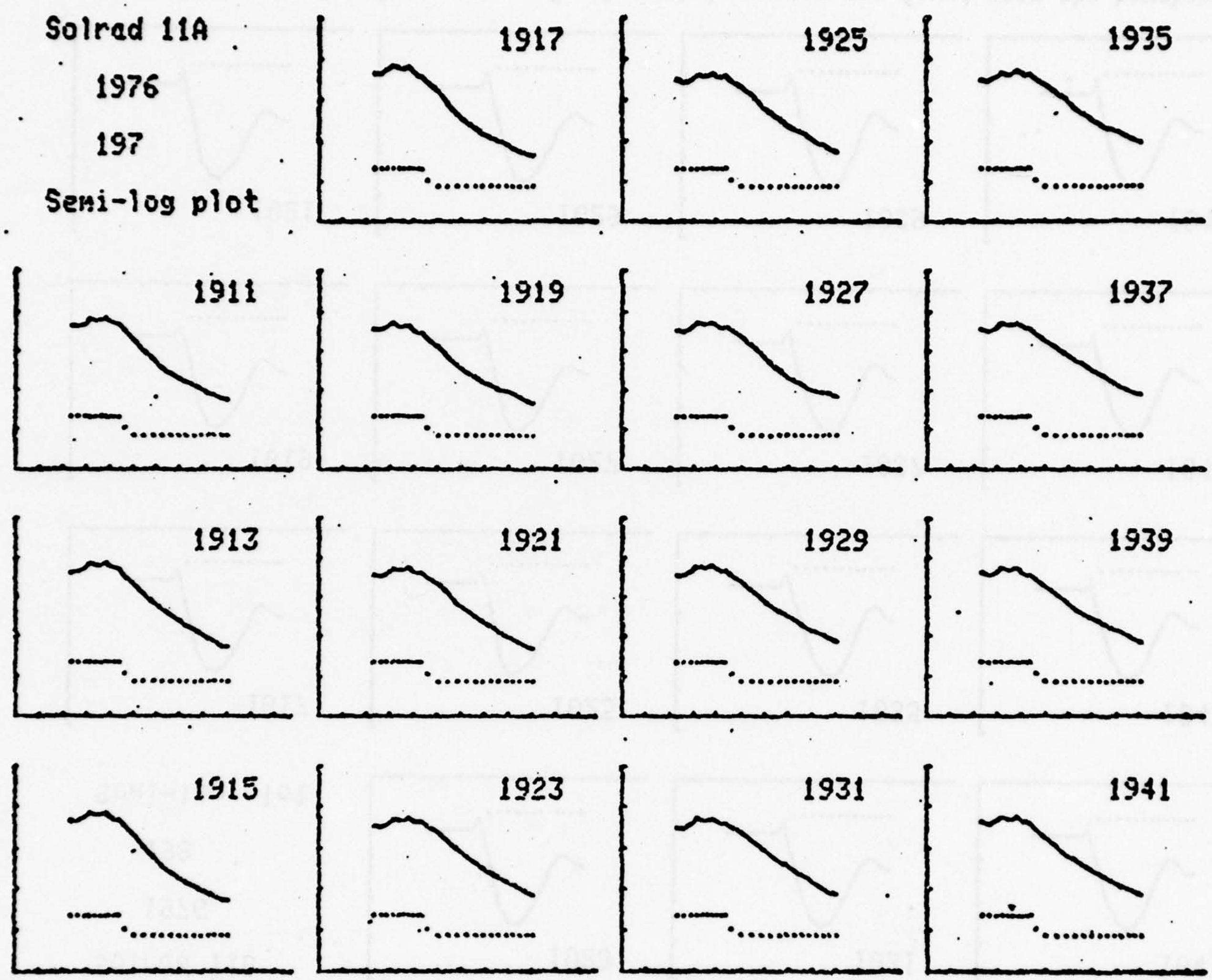

A series of magnetosheath spectra found away from the bowshock.

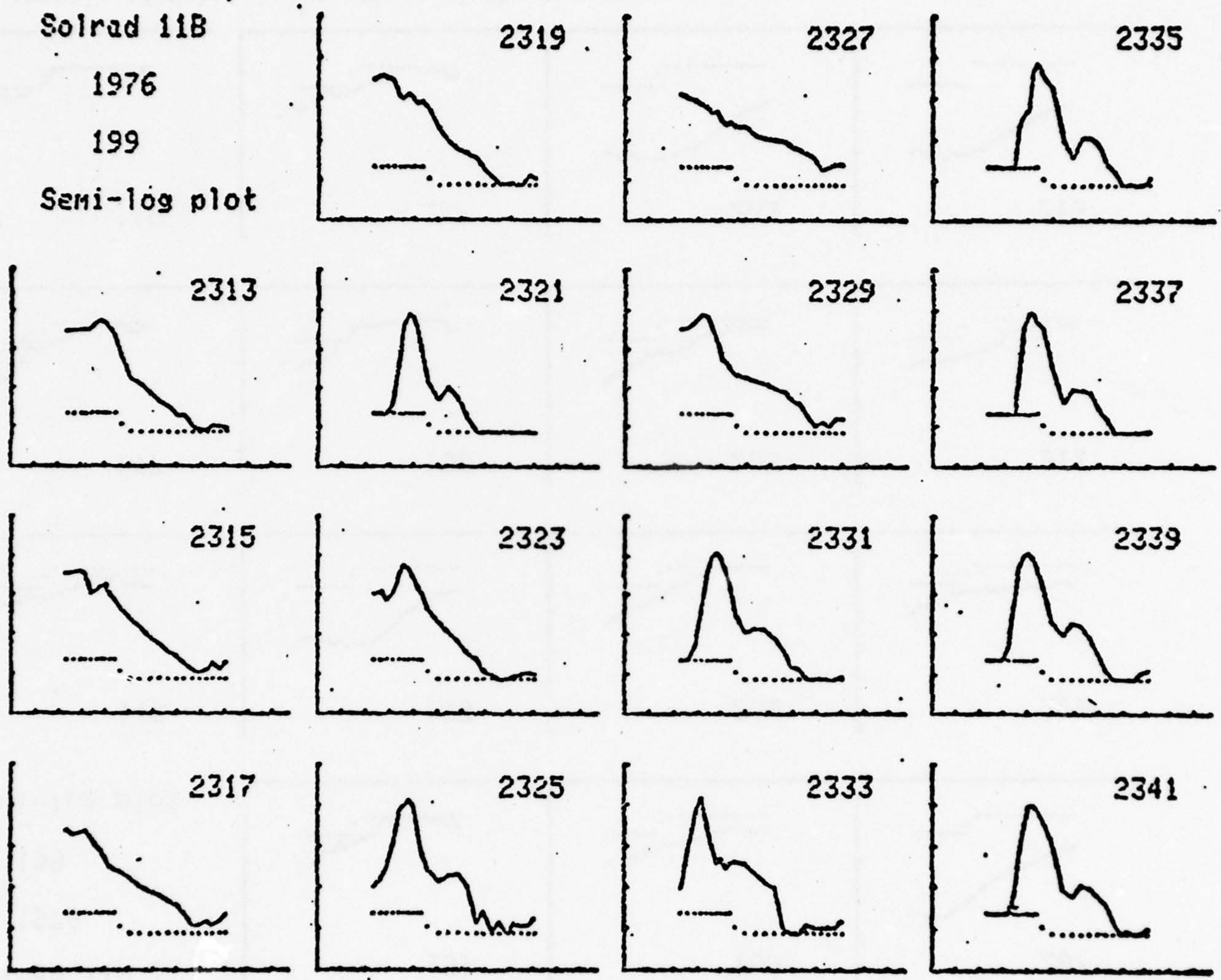

Samples taken from within a multiple bowshock crossing event.

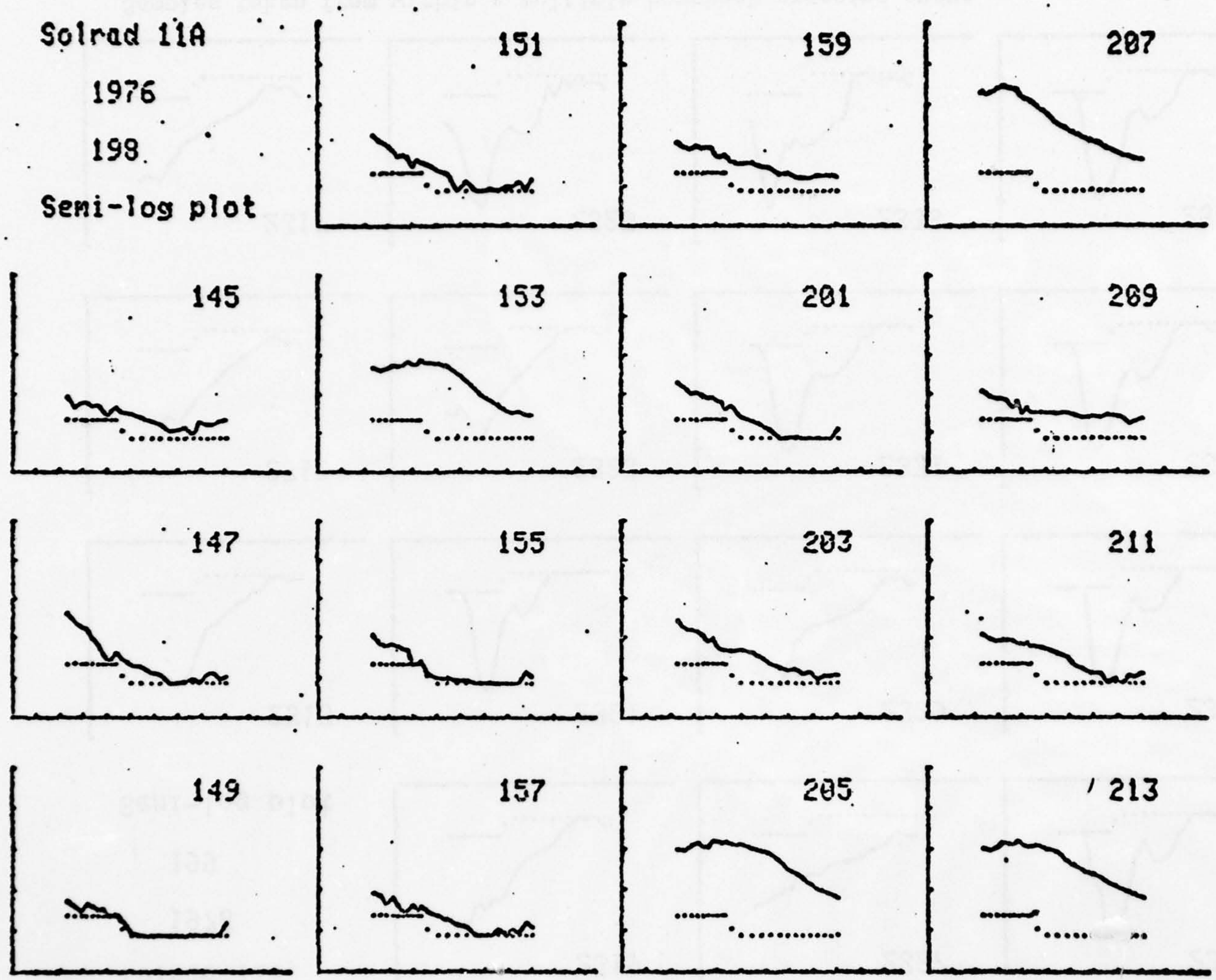

An example of multiple crossings of the magnetopause.

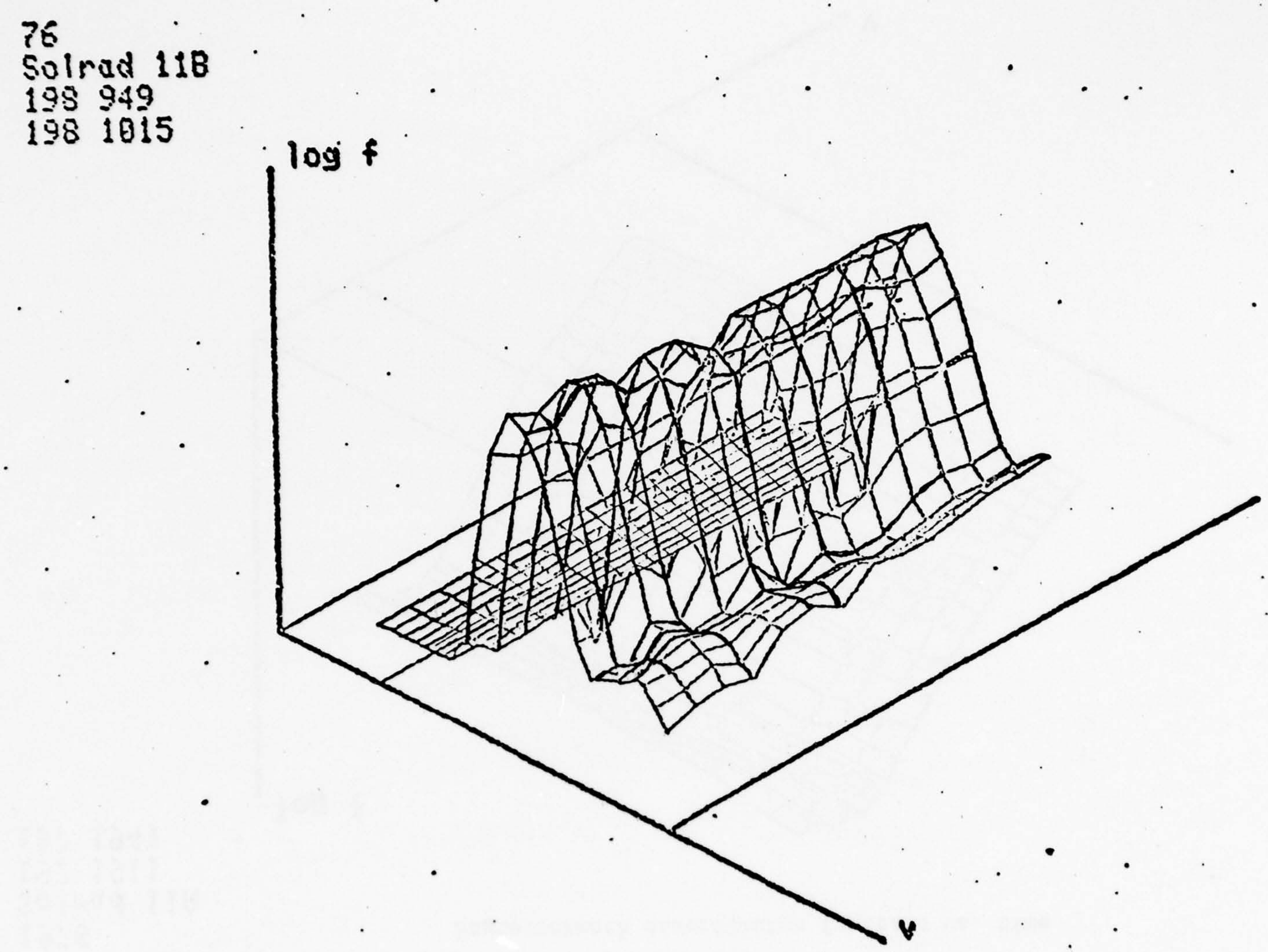

Plasma distribution spectrum vs. time for a solar wind sample.

1976
Solrad 11A
197 1911
197 1941

Magnetosheath distribution function vs. time

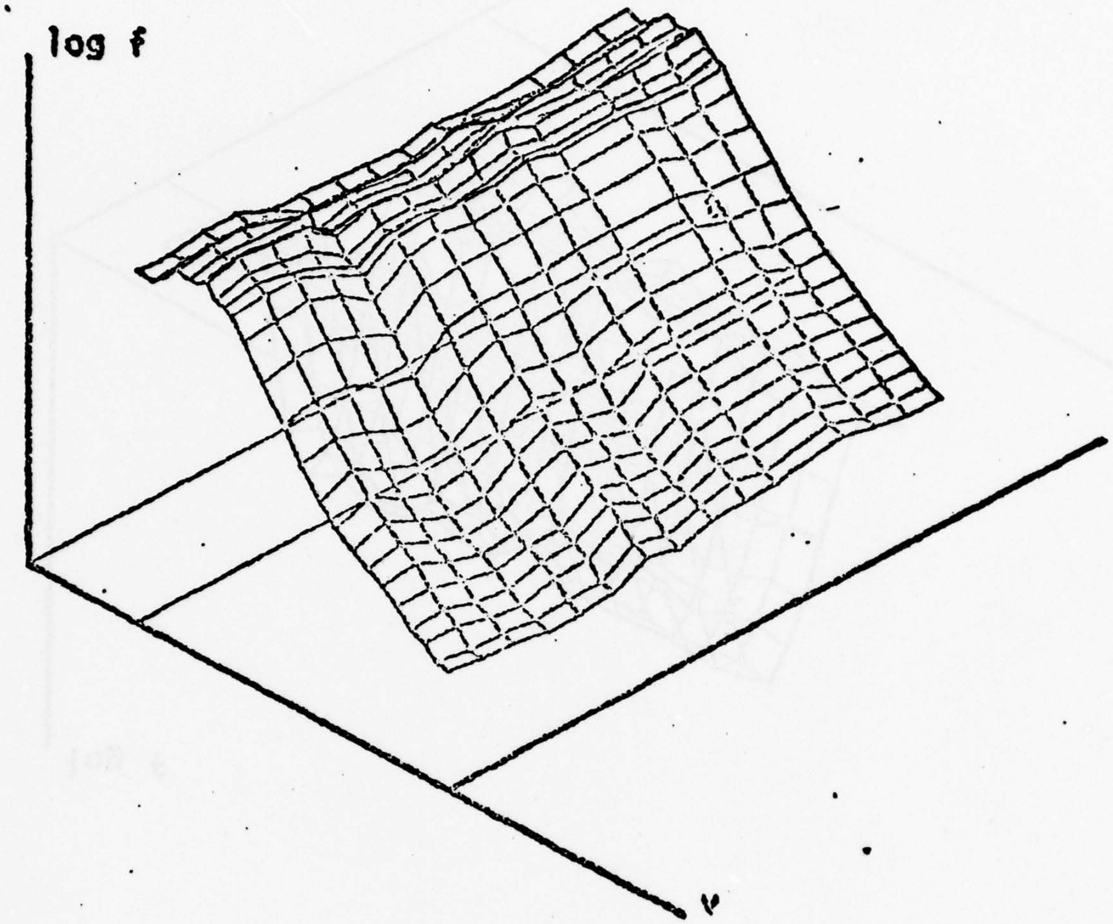

1976
Solrad 11B
199 1929
199 1957

Distribution function vs. time for a section of a multiple shock crossing

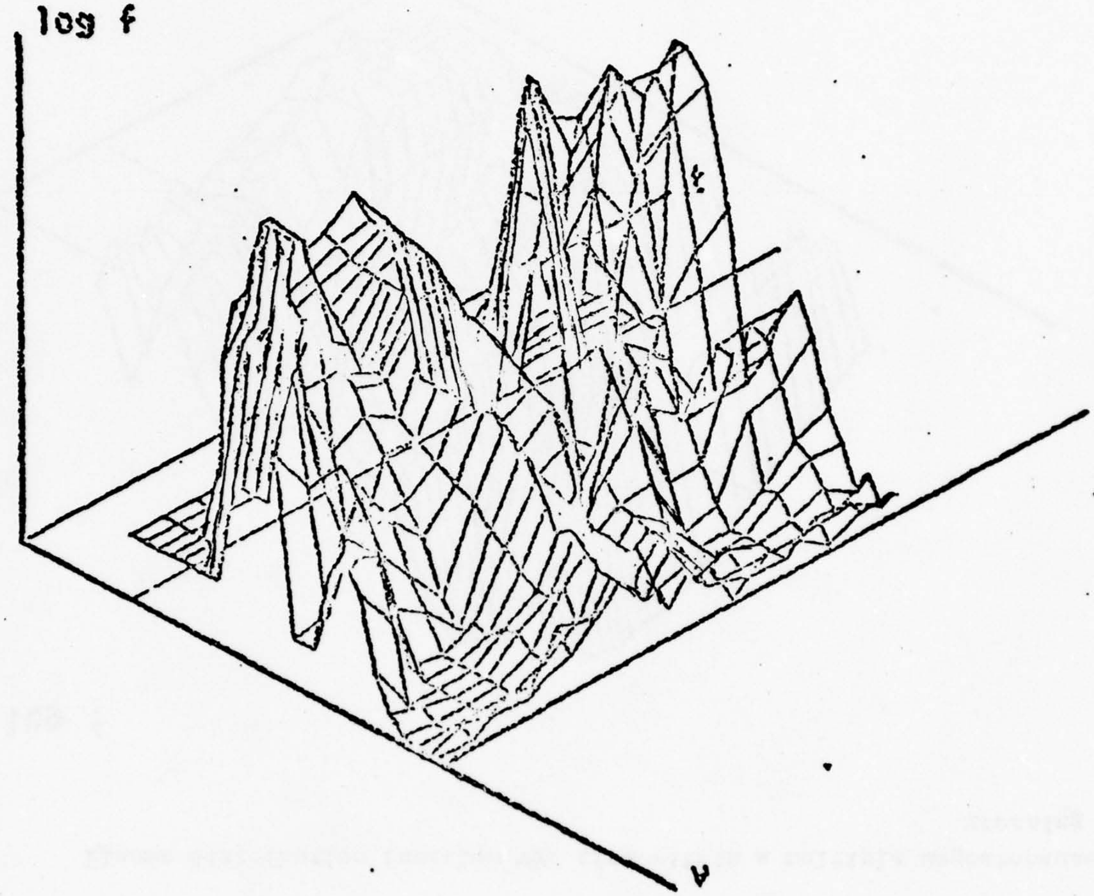

1976
Solrad 11A
198 145
198 213

Plasma distribution function vs. time within a multiple magnetopause crossing

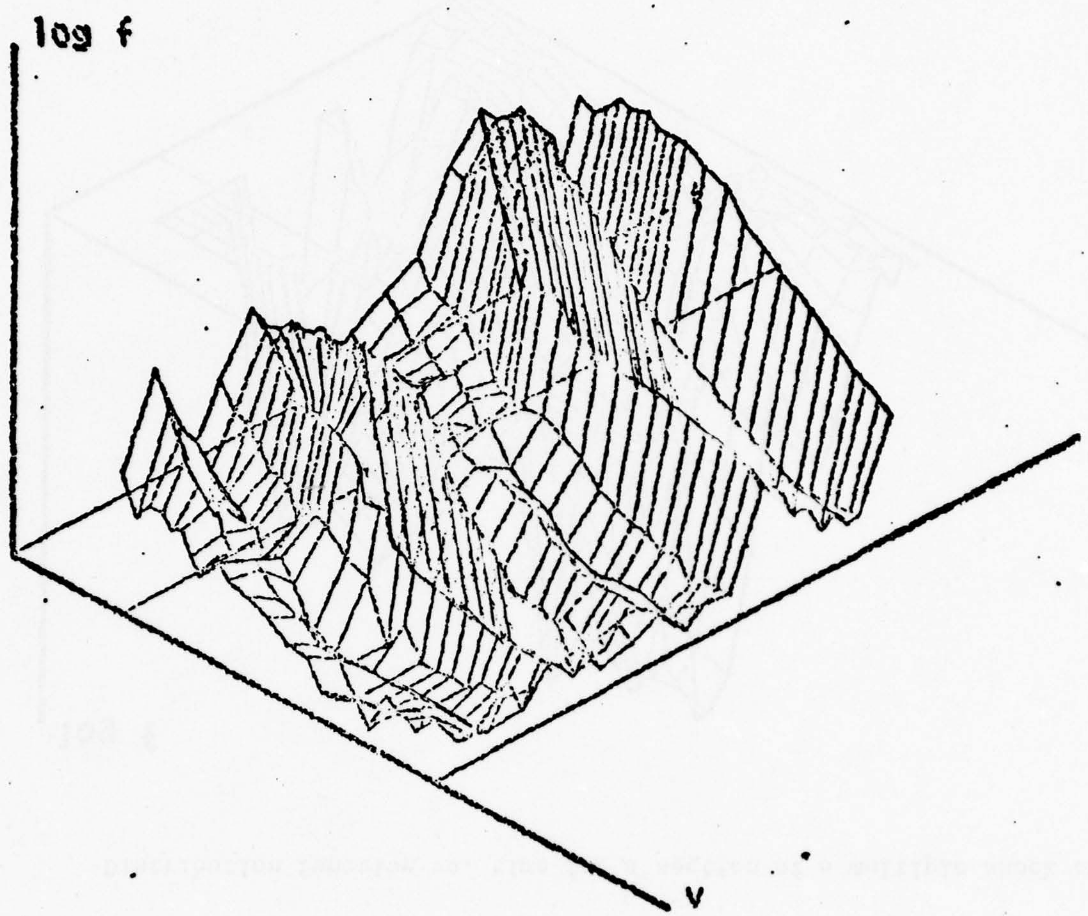

CHAPTER THREE

SOLRAD'S 'ANALYSIS' PROGRAM

The purpose of the 'Analysis' program is to return values of the plasma parameters of z-component of bulkspeed (SPEED), density (DEN), most probable thermal speed (THSP), and the temperature (TEMP), and provide the values of angles, including THETA, the angle of incidence, involved in the analysis, from the original data tape. The WIND subroutine of this program provides the derivation of these four parameters by rough numerical integration of the zeroeth, first, and second moments of velocity. These integrations are done over a significant portion of the distribution function, where the limits must be determined by the position of the peak channel of the distribution.

The variable F(J) used by the program is proportional to a 'differential density' of the plasma. It is defined as the current in the Jth channel divided by the average velocity detected by the channel. That is,

$$F(J) = \frac{CURR(J)}{V(J)} = \frac{CURR(J)}{\frac{1}{2}(v1+v2)}$$

for v1 and v2 the velocity limits of the channel. This equals the density of only those particles within the energy limits of the channel times the charge per particle times the area of collector plate illumination.

The distribution function's average value in the nth channel equals

$$f_n = \frac{k\ CURR(J)}{(q/m)\Delta E_J} \propto \frac{CURR(J)}{\frac{1}{2}(v2-v1)(v2+v1)} \propto \frac{F(J)}{\Delta V_J}$$

as is expected from the definition of distribution function ($f=\partial n/\partial v$) and F(J) for ΔE_J the energy width and ΔV_J the velocity width.

The program wrongly seeks the channel of highest F(J), which varies as the distribution function only when the velocity width is constant.

```
FORTRAN IV G LEVEL  21                    WIND                 DATE = 77123          21/41/29

      SUBROUTINE WIND(SPEED,DEN,THSPD,TEMP)
      COMMON DN(33),CUR(33)
      DIMENSION F(33)
      INTEGER DN
      DATA C1,C2,C3,C4,C5/2.44E-13,1.0367,1.0,125.0,1.86E+12/
      DATA X2/0.964594/
      DIMENSION VOLTLO (26),VOLTHI(26),V(26)
      DATA VOLTLO /0.0,240.8,314.7,395.7,473.6,549.9,610.0,705.1,781.7,8
     $61.5,938.2,1015.9,1171.3,1405.3,1640.7,1878.0,2115.5,2351.7,2591.1
     $,2831.3,3072.8,3314.4,3556.4,3800.6,4045.0,240.5/
      DATA VOLTHI /0.0,319.3,396.6,476.8,551.6,627.2,707.8,783.1,859.5,9
     $39.7,1016.1,1171.7,1406.1,1639.7,1875.1,2111.2,2348.4,2587.0,2826.
     $0,3067.3,3305.7,3548.3,3789.2,4033.1,4278.7,4279.5/
      LOGICAL FIRST/.TRUE./
      IF(.NOT.FIRST) GO TO 6
      Q = 1.6021E-19
      REM = 1.67252E-27
      SQM = SQRT(2*Q/REM)
      DO 2 J=2,26
      V(J) = SQM*(SQRT(VOLTHI(J))+SQRT(VOLTLO(J)))/2000.0
    2 CONTINUE
      FIRST=.FALSE.
    6 CONTINUE
      DO 10 J = 2,33
      IF(DN(J).GT.256) GO TO 50
C     C1=2.44E-13
C     IF(J.GE.26) C1=2.22E-13
C     IF(J.GE.30) C1=6.94E-13
C     CUR(J) = C1*(C2**FLOAT(255-DN(J)))
C     X1=C1*C2**255
C     X2= 1.0/C2
C     9/13/76-VALUE OF X1(WORDS 2-25) CHANGED FROM 2.39293E-9.
C     X1(WORDS 30-33) CHANGED FROM 6.80612E-9. X1(WDS 26-29) UNCHANGED.
C     THIS CALIBRATION CHANGE IS EQUIVALENT TO CHANGING ABOVE VALUES
C     OF C1 TO 6.94E-13(WDS 2-25) AND 2.74E-12(WDS30-33).
      X1=6.80612E-9
      IF (J.GE.26) X1=2.17717E-9
      IF (J.GE.30) X1=2.68842E-8
      CUR(J)=X1*X2**DN(J)
      IF (J.GT.25) GO TO 10
      F(J)=CUR(J)/V(J)
C  V(J) IS THE AVERAGE SPEED FOR CHANNEL J IN KM/SEC.
   10 CONTINUE
      M = 2
      DO 20 J = 3,25
      IF (F(J).GT.F(M)) M = J
   20 CONTINUE
      LL = M-3
      LU = M+3
      IF (LL.LT.2.OR.LU.GT.25) GO TO 50
      S0 = 0.0
      S1 = 0.0
      S2 = 0.0
      DO 30 J = LL,LU
      S0 = S0+F(J)
      S1 = S1+V(J)*F(J)
      S2 = S2+V(J)*V(J)*F(J)
   30 CONTINUE
      SPEED = C3*S1/S0
      TEMP = C4*((S2/S0)-SPEED**2)
      DEN = C5*S0
      THSPD= SQRT(2*TEMP/C4)
      RETURN
   50 SPEED = -100.
      TEMP = -100.
      DEN = -100.
      THSPD=-100.
      RETURN
      END
```

For the solar wind samples, consecutive channels near the proton peak vary to a greater extent than in a magnetosheath sample. This large variation overcomes any effect from not considering the distribution function and none of the solar wind spectra seem to be affected by the error. In the magnetosheath, however, with greater thermal speeds, the distribution function varies less between adjacent channels so that this error often causes the computed bulk velocity to be greatly shifted to the right, to a velocity within or near those associated with the 12th or 13th channel where the energy width increases and therefore the velocity width changes the greatest amount from the channel one below it in energy. Lines 30 to 31 of the program determine the peak of F(J).

The region of integration is taken to be from three channels below to three channels above the maximum flux channel (channel M) if these channels exist (see line 35). In the required integrals, the correct summation expression involves the current flux. Consider the density.

$$\int_{v_{M-3}}^{v_{M+3}} F(v)dv \propto \Sigma f_n \Delta v_n \quad \text{and therefore} \quad \int F(v)dv \propto \Sigma F(J).$$

Thus it is the following summations that are calculated in lines 36 to 46.

$$\text{DEN} = C_5 \; \Sigma F(J)$$

$$\text{SPEED} = \frac{C_3 \; \Sigma V(J)F(J)}{C_5 \; \Sigma F(J)}$$

TEMP and THSP are calculated from DEN, SPEED, and the second moment $\Sigma \, V^2(J)F(J)$.

The Σ represents summation over the seven chosen energy windows.

When the analysis is applied to the magnetosheath, two other problems arise. First, the maximum flux channel is found too close in energy to the lower energy limit of the apparatus so that the M-3 channel does not exist (as a proton channel). This is because the plasma's z-component of bulk velocity is considerably decreased (by approximately a factor of two), from the geometry of the bowshock and its mechanism of collision, from its previous value out in the solar wind. The analysis program does not attempt to determine any parameter and returns a -100. for each as can be seen in the data.

The second problem with magnetosheath spectra is that there is a greater error in the density calculation because the seven energy channels are not as sufficient as for the solar wind samples.

To provide a means to test this analysis, the Solrad 'Currents' program was developed so that currents expected in each channel could be derived from the plasma parameters. In the next two chapters can be seen the comparisons between the observed currents and those expected from the determined parameters.

CHAPTER FOUR

SOLRAD'S 'CURRENTS' PROGRAM

Description of 'Currents' program

The currents program simulates the datanumbers that correspond to the twenty-four contiguous positive-ion energy channels and one large energy channel from the given information of plasma z-component of bulk velocity, most probable thermal speed, and number density.

The current from each channel is computed by a three-dimensional integration over velocity space. As we presently do not consider predicting the separate currents from each of the three sectors, the symmetry of the detector lends itself to a two-dimensional consideration. However, this program was adapted for Solrad and it was originally required to consider the three velocity components separately.

In addition to calculating the current expected from the direct effect of grid modulation, the program takes into account a refraction effect. This is caused from a greater particle refraction with the impressed grid modulation at VHI volts than at VLOW volts (for VHI and VLOW the upper and lower limits of the square wave voltage).

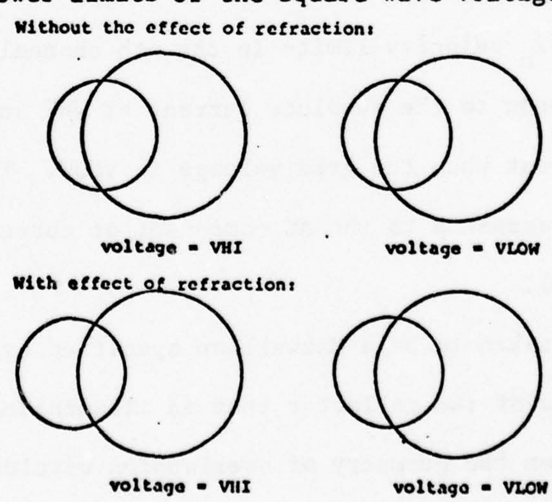

As the grid voltage varies, so does the collector current, at 180° out of phase. The refraction effect subtructs a greater amount of collector plate DC current at grid voltage VHI than at grid voltage VLOW when the plasma image of the aperture does not fall entirely on the collector. This is because, at a non-zero angle of incidence, the center of the aperture image is displaced by a greater amount from the center of the collector at VHI and the plasma would illuminate a smaller part of the collector, as shown in the previous diagram.

Integrating v_z between the limits of the considered channel calculates only the current not produced by the refraction effect. To take it into consideration v_z must be integrated out to positive infinity, since all velocities greater than the threshold velocity (for entering the grids) can contribute to the refraction effect. The necessary integration, performed numerically in this program is as follows (using the notation from page 5):

$$I_n = \tau qn\left(\left(\iiint v_z f(\vec{v})A(\vec{v})\,dv_x\,dv_y\,dv_z\right)_{V=VHI} - \left(\iiint v_z f(\vec{v})A(\vec{v})\,dv_x\,dv_y\,dv_z\right)_{V=VLOW}\right)$$

for $v1_n$ and $v2_n$ velocity limits in the nth channel, since the first term corresponds to the absolute current at VHI and the second to the absolute current when the grid voltage is VLOW. The difference of these two terms corresponds to the AC component of current expected (CURR(NCHAN) for NCHAN = n).

$f(\vec{v})$ is taken to be a Maxwellian specified by the input parameters. $A(\vec{v})$, the area of the collector that is illuminated by the plasma, is calculated from the geometry of overlapping circles. A full description of the program can be read in Appendix A.

The 'Currents' program yet does not consider the effect of alpha particles. If the analysis program were to be modified to determine the proportion of alpha particles in a spectra and roughly their thermal speed, the consideration of alpha-particles by 'Currents' would be an immediate consequence.

Computational results

To determine how closely the 'Analysis' program and 'Currents' program are inverse 'functions', the WIND subroutine was made into 'Wind2' so as to accept the datanumbers punched on cards by 'Currents' and analyze the produced currents. By inputting into 'Currents' a set of parameters, any deviation from these in the output of 'Wind2' is then noted.

Results showed that the velocity correlation is phenomenal, to within .8% when thermal velocities reasonable for the solar wind are considered.* A fairly large discrepancy is found with density and thermal speed. The density discrepancy, as expected, increases as thermal speed is increased. For $v_z = 400$ km/s and thermal speed equal to 50 km/s, density is off by only about 2%.† However, a thermal speed of 100 km/s reduces the density by almost a factor of two and the thermal speed is off by -38%. Apparently the 'Analysis' program is not integrating over a sufficiently large range of the distribution function. A further analysis of this problem is necessary with regards to modifying the analysis program to enable a more accurate analyzation of the magnetosheath spectra.

* Velocity is off by as much as 12% for thermal speed = 100 km/sec.

† Thermal speed is off by about 8%.

Graphic Results

For comparison, the Techtronix 4051 graphics system was used to plot the distribution function computed from the datanumbers produced by 'Currents' on the same graph as that derived from the original data.

The following pages show the original data in dots or (+) and the expected distribution from the 'Currents' program with a solid curve. The discrepancies talked about in Chapter Three concerning the magnetosheath samples are evident from these plots. That the 'Analysis' program was not designed to properly analyze magnetosheath data is apparent. When the lower energy distribution values do not vary rapidly enough the curves are found to shift to center around the 12th or 13th channel. This can be noted from the linear plot on page 32. From this it is apparent that the error is large.

The solar wind spectra match very well in all parameters with a slight discrepancy again observed in density.

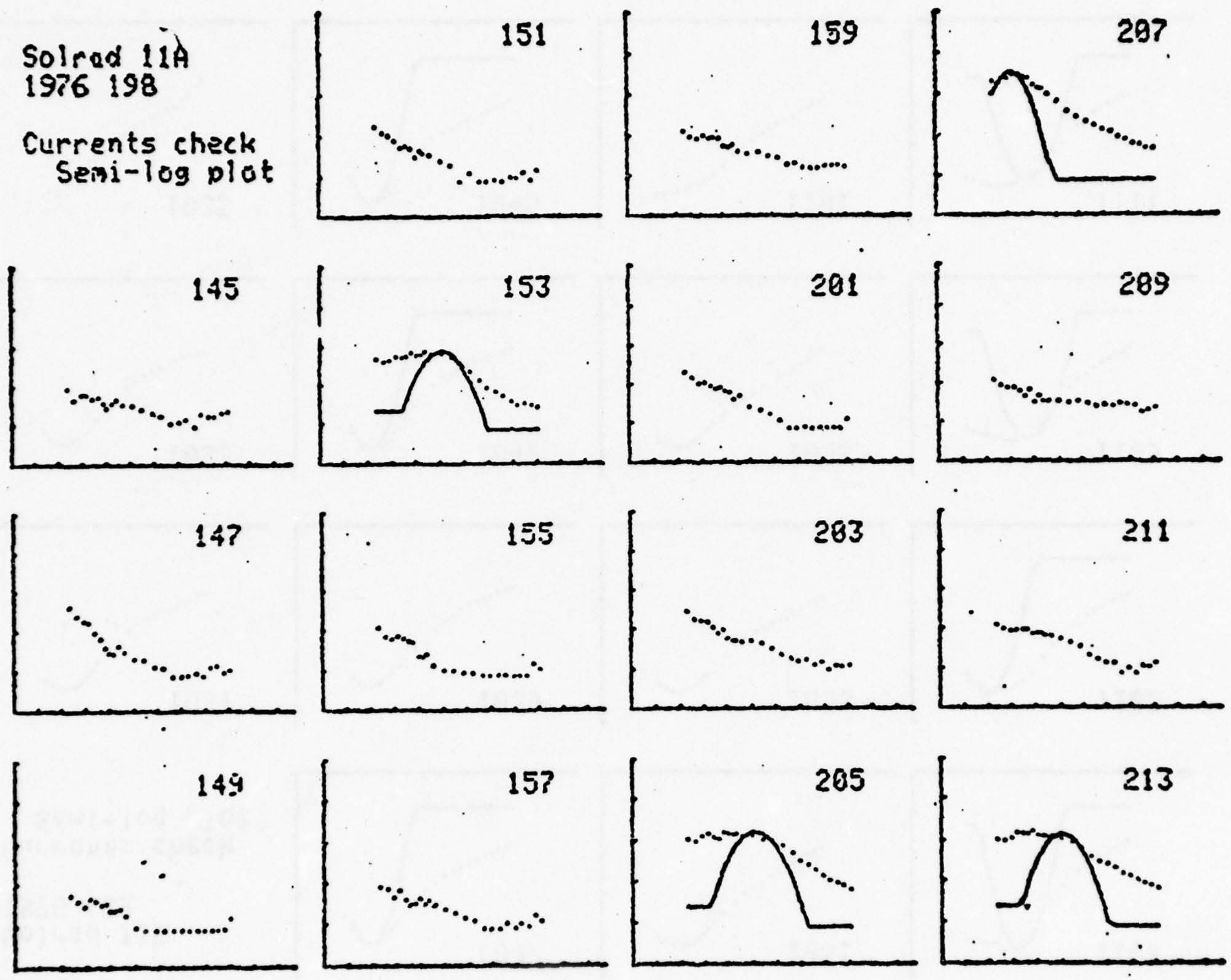

Solrad 11A
1976 198
Currents check
Semi-log plot
151
159
207
145
153
201
209
147
155
203
211
149
157
205
213

Solrad 11B
1976 182

Currents check
Semi-log plot

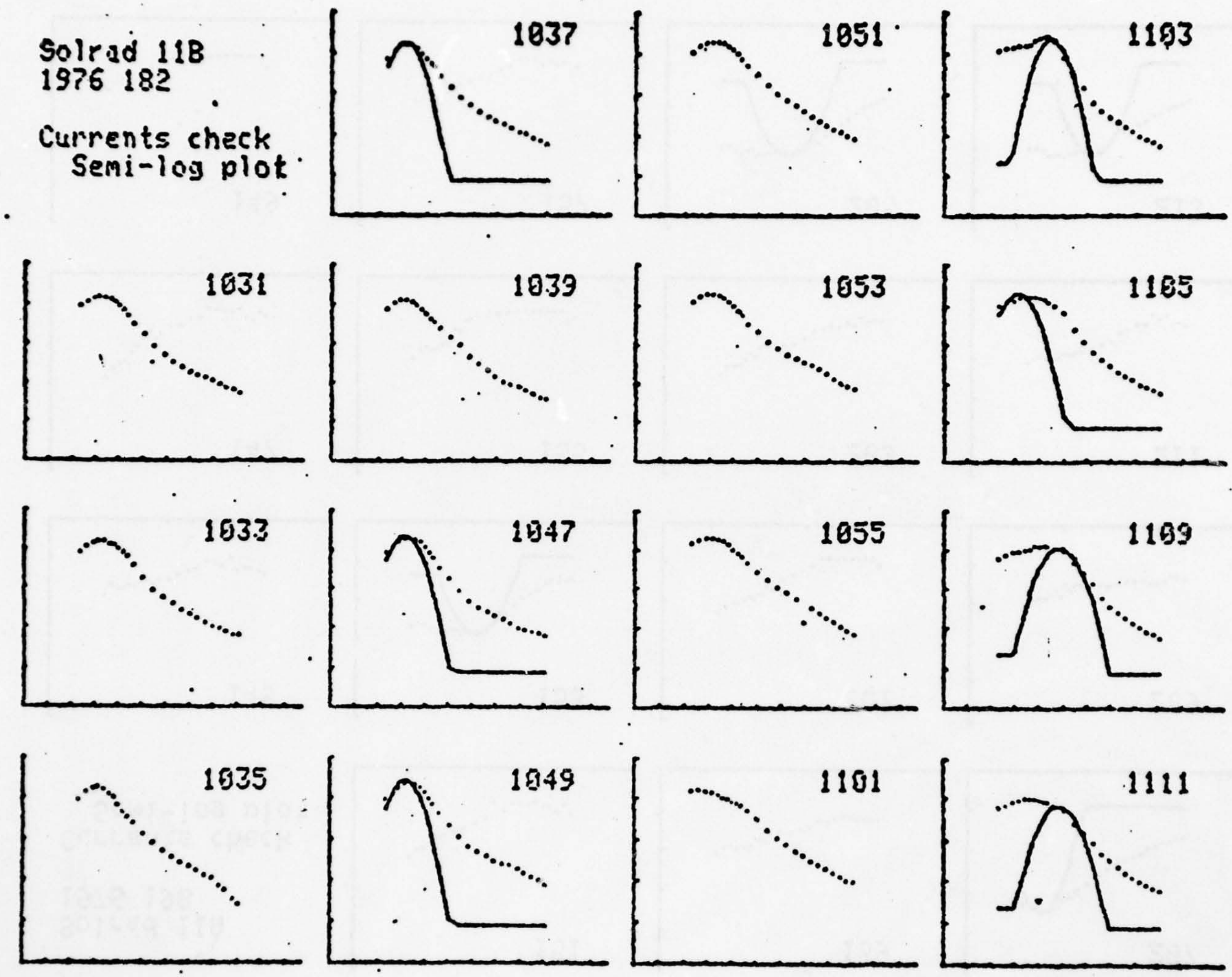

Solrad 11B
1976 198

Currents check
Semi-log plot

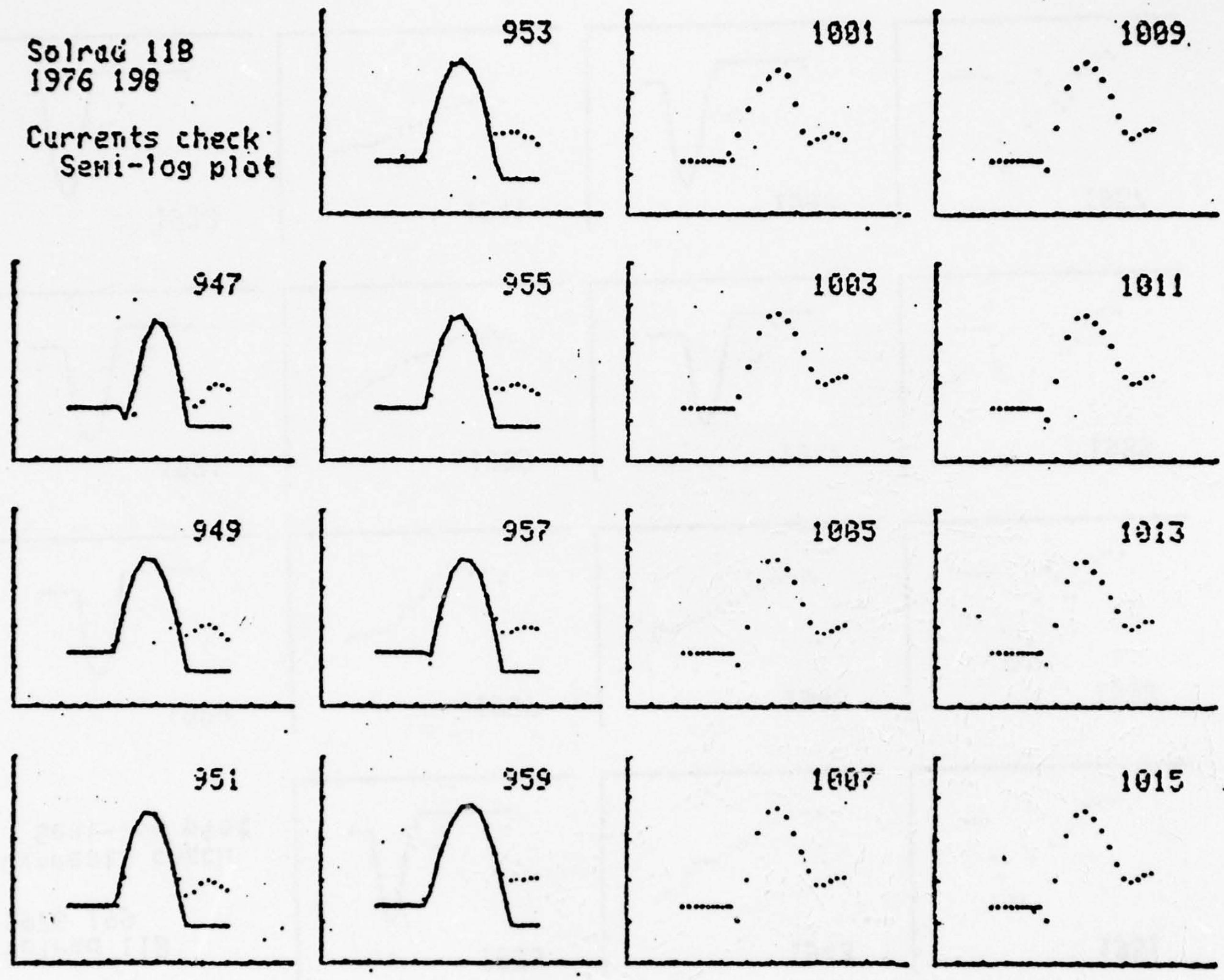

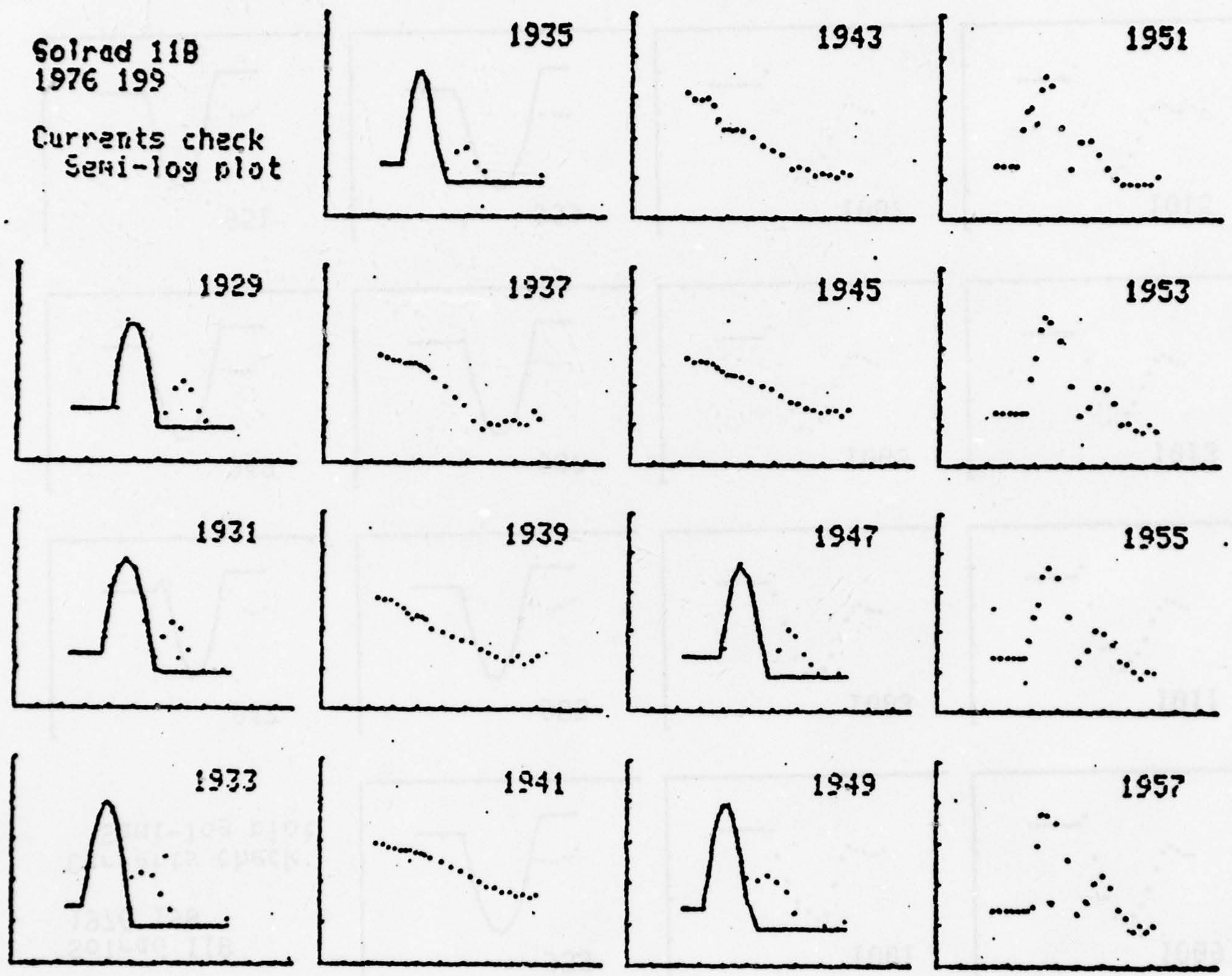
Solrad 11B
1976 199
Currents check
Semi-log plot
1935
1943
1951
1929
1937
1945
1953
1931
1939
1947
1955
1933
1941
1949
1957

Solrad 11A
1976 197

Currents check
Semi-log plot

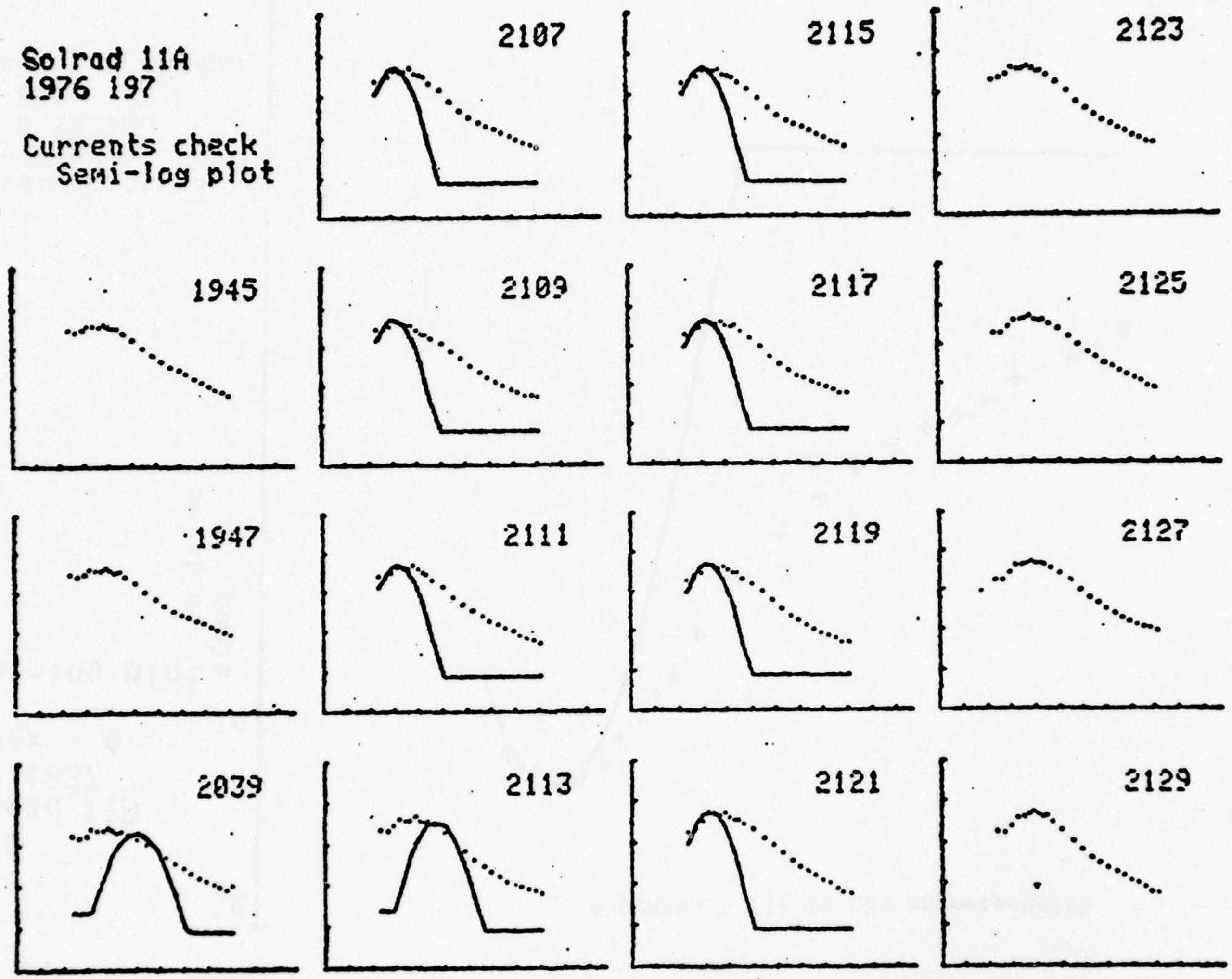

note: scale is explained on page

1976
Solrad 11B
192 1837
index = 4

Semi-log plot

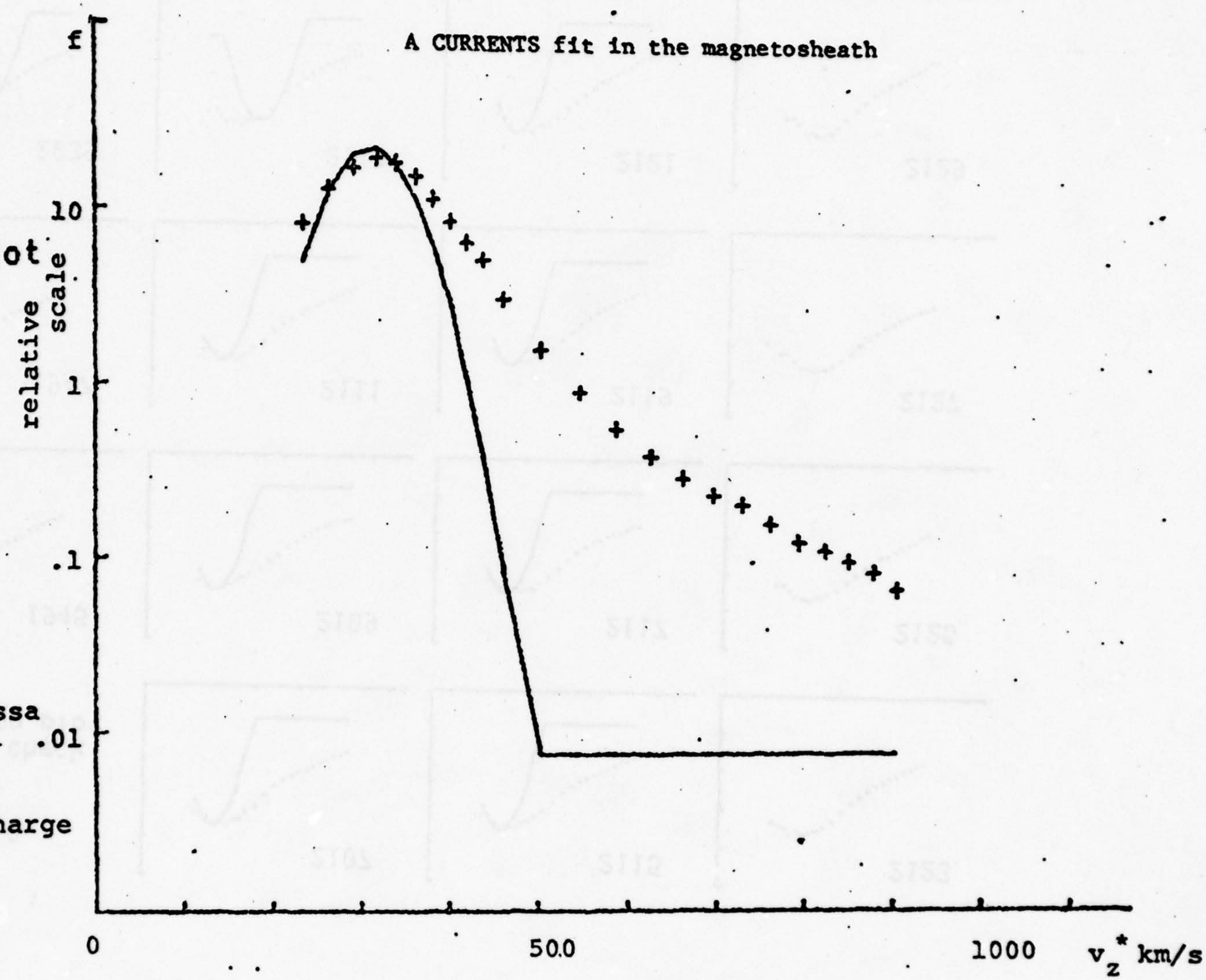

* note: abscissa is $v_z\sqrt{(m/q)}$ for m in amu and q in elementary charge

1976
Solrad 11B
192 1111
index = 15

* note: abscissa
is $v_z \sqrt{(m/q)}$
for m in amu
and q in
elementary charge

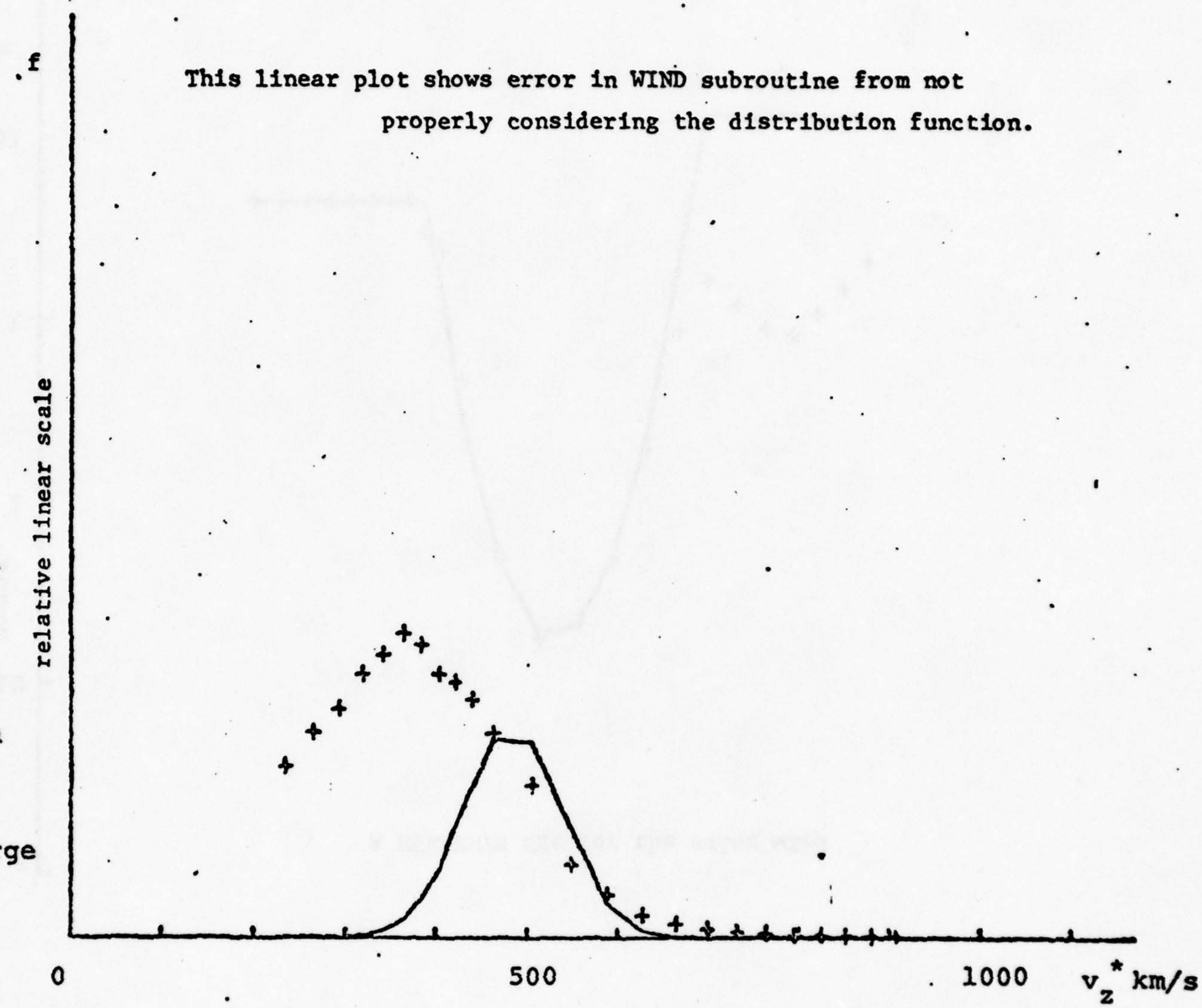

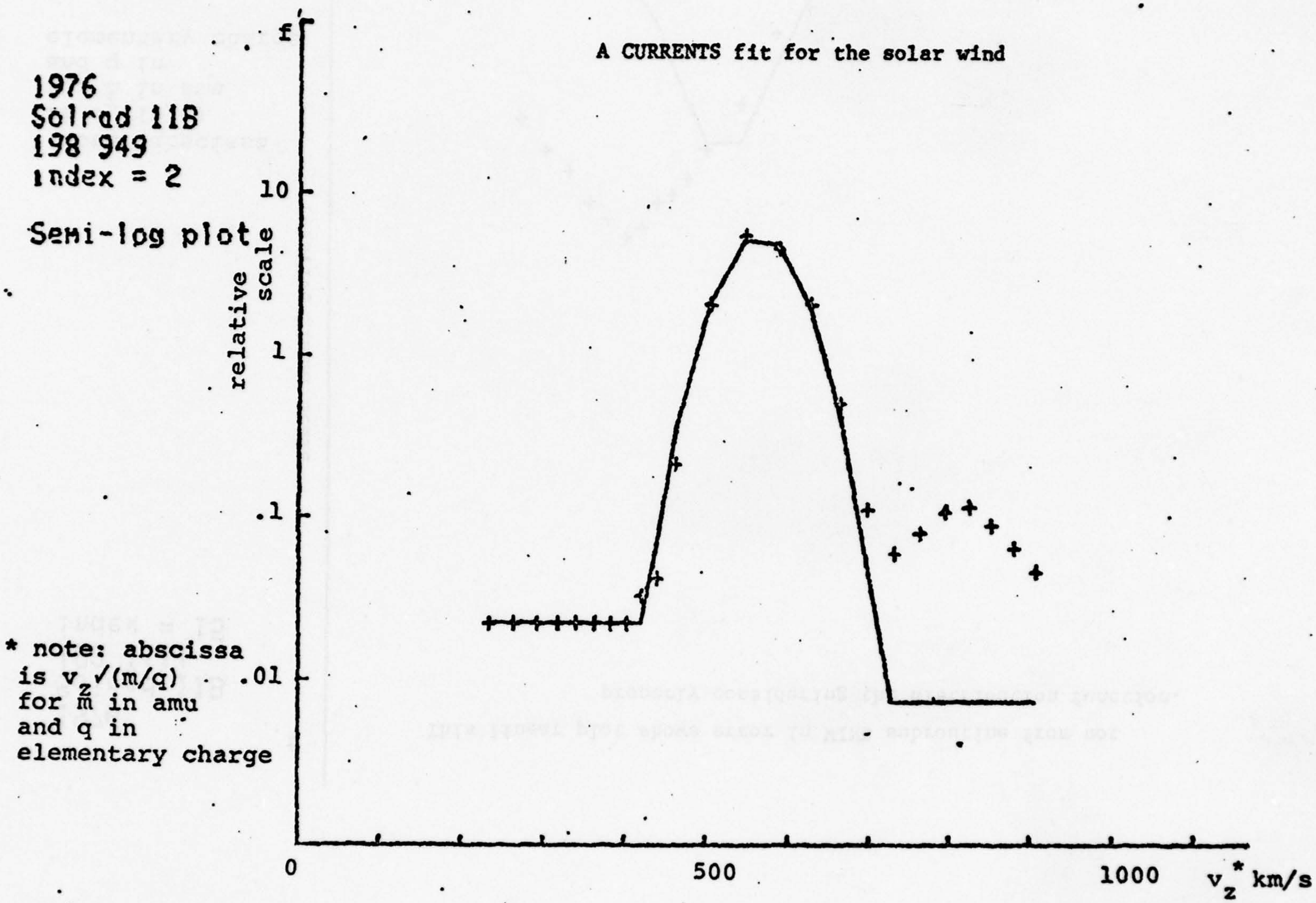
A CURRENTS fit for the solar wind
1976
Solrad 11B
198 949
index = 2
Semi-log plot
f
relative scale
10
1
.1
.01
0
500
1000
v_z^* km/s
* note: abscissa is $v_z\sqrt{(m/q)}$ for m in amu and q in elementary charge

CHAPTER FIVE

GRAPHIC KAPPA AND MAXWELLIAN FITS

The Techtronix graphics display can also be used to make an analysis of the spectra by plotting a theoretical distribution function of v_z, whose parameters are determined by trial and error, that fits the observed function.

Each parameter of a Maxwellian or Kappa distribution function can be changed by using a 'user definable key' on the console.

The Kappa velocity distribution is of the following form:

$$f(\vec{v}) = \frac{n}{\pi^{3/2}\omega_o^3} \frac{\Gamma(\kappa+1)}{\kappa^{3/2}\Gamma(\kappa-\frac{1}{2})} \left(1+\frac{|\vec{v}-\vec{vbulk}|^2}{\kappa\omega_o^2}\right)^{-(\kappa+1)}$$

This distribution function is thought to provide a good fit for spectra in the magnetosheath. The Kappa distribution, which is a statistical sum of Maxwellians, has one more adjustable parameter than the Maxwellian, the value of kappa. The following page shows a Kappa speed distribution (where the velocity distribution function is multiplied by $|\vec{v}-\vec{vbulk}|^2$) for cases of kappa equals one to five and infinity. A Kappa distribution for kappa equals infinity is a Maxwellian. The graph on the left shows each curve relatively normalized while the one on the right sets each peak at a constant value. As is most evident from the righthand plot, the Kappa distribution has a high energy tail, although its velocity distribution is symmetric.

Since in Solrad we can only deal with the z-component of velocity, a speed distribution analysis is not possible. The velocity distribution must be reduced to a one-dimensional distribution by integrating over all v_x and v_y. The result, without calculating the normalization C is:

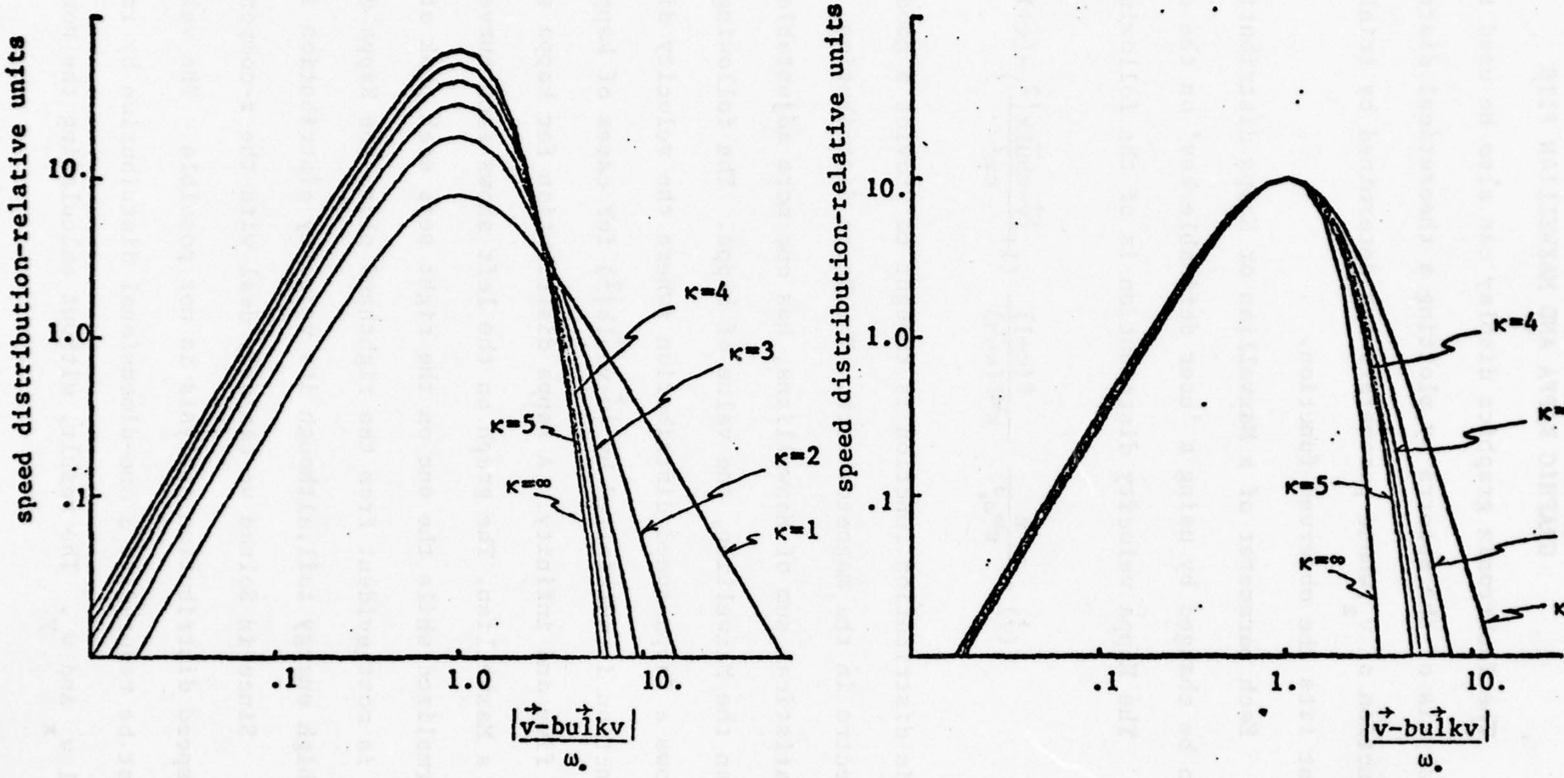

Speed distribution for Kappa plotted. Lefthand graph is relatively normalized.

$$f(v_z) = \frac{C}{\left(1+\frac{v_z^2}{\kappa\omega_o^2}\right)^{\kappa}}$$

For ease in fitting the data, the maximum is constrained to one value (determined by one user's key). Thus, what is plotted is:

$$f(v_z) = C(1+\frac{1}{\kappa})^{\kappa}/(1+\frac{v_z}{\kappa\omega_o^2})^{\kappa}$$

Density, although the parameter is printed next to the graphs, was not used as an adjustable parameter in obtaining the Maxwellian or Kappa fits.

Results

The results are promising. Magnetosheath examples are shown in pages 40 to 45 . It is interesting to note that spectra taken near each other in time each have very closely the same relation to the closest curve obtained as a fit.

The day 198 hour 205 spectrum on page 42 shows a magnetosheath sample taken from very near the magnetopause.

Page 43 shows a case that seems to have kappa less than two.

Because of the alpha particle peak, the spectra fits were attempted around the proton peak and the highest energy points. This is only justified when the sum of alpha and curves converges with the proton curve at high energies. To determine whether or not this convergence exists, the program was modified so that alpha particles would also be considered. Page 44 , day 182 hour 1101 shows each component separately together with their sum. It is seen to have the convergence necessary although a better fit could be obtained.

A closer fit for the alpha particles, however, seems to indicate (page 45) a smaller thermal speed which would conserve the convergence. However it is seen that with a larger alpha-particle thermal velocity, the convergence does not exist. A deeper analysis of this convergence problem is warranted.

It is worth remembering at this stage what initial assumptions were made for the distribution function to be calculated in the plotting programs. It is important to check that that the error resulting from approximations in the derivation of the formula used does not so greatly affect the accuracy of each point that the curve fitting analysis would not be valid.

For this purpose the 'Currerr' program was devised. It is the 'Currents' program, modified so that the AREA array alternates between describing the exact area response function and an ideal flat response function (where each element of AREA ≡ ANORM). The current values are measured at each channel with each response function and the percentage deviation, of the currents calculated with the exact-area response function from the currents calculated with the ideal response function, is determined.

These values would then give an indication as to the error resulting from considering the area constant (i.e. a flat response) in the plotting program. The bulkspeed was considered at 500 km/s at normal incidence on the detector and density at 5/cc. Thermal speed was varied between 75 and 250 km/s to observe the relationship between the error of current in a channel and the quantity w/v_z.

As we consider calculations for higher thermal velocities, the largest current deviations are found in the low energy channels where it appears that the expected current is very low but the refraction effect is relatively high (since it is due to particles of energy greater than that representative of the channel). There exists a very low deviation in the high energy channels perhaps since the refraction effect involves much fewer particles.

The negative deviation in low energy channels for low thermal speeds is yet to be understood.

What is evident from the results of this program is that the current deviation in the high energy channels is very small, as for example to within 1% for channels 16 to 25 for the 150 km/s thermal speed case. This is important to note when considering distribution fits through the high energy points. The low energy points may, owever, be significantly be affected by choice of response function.

The 'Currerr' program, it should be kept in mind, might need to be revised since the AREA array is not the only thing in the program that sets a limit to the response function actually determined in 'Currents'.

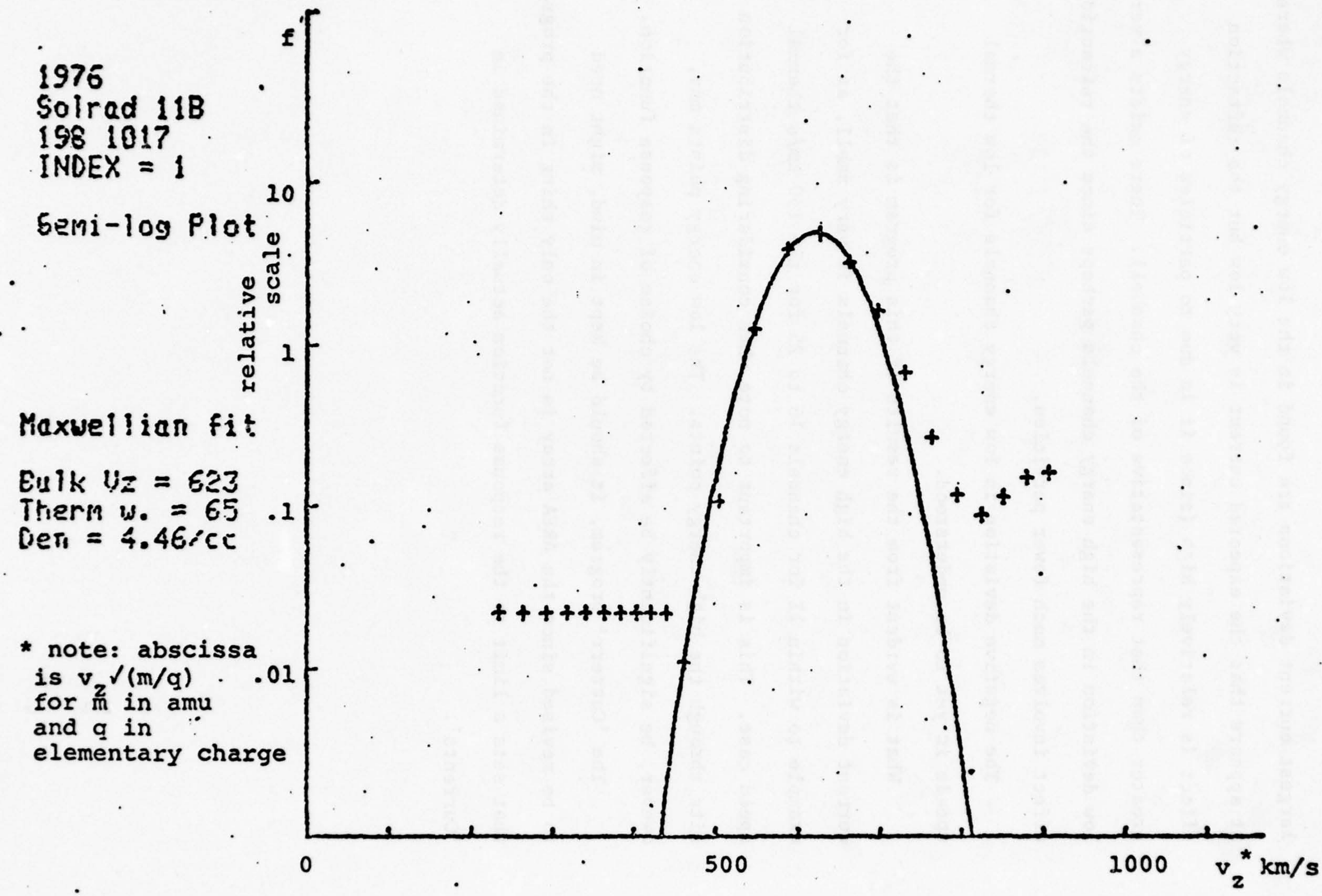
1976
Solrad 11B
198 1017
INDEX = 1
Semi-log Plot
Maxwellian fit
Bulk Vz = 623
Therm w. = 65
Den = 4.46/cc
* note: abscissa
is $v_z\sqrt{(m/q)}$
for m in amu
and q in
elementary charge
f
10
1
.1
.01
relative scale
0
500
1000
v_z^* km/s

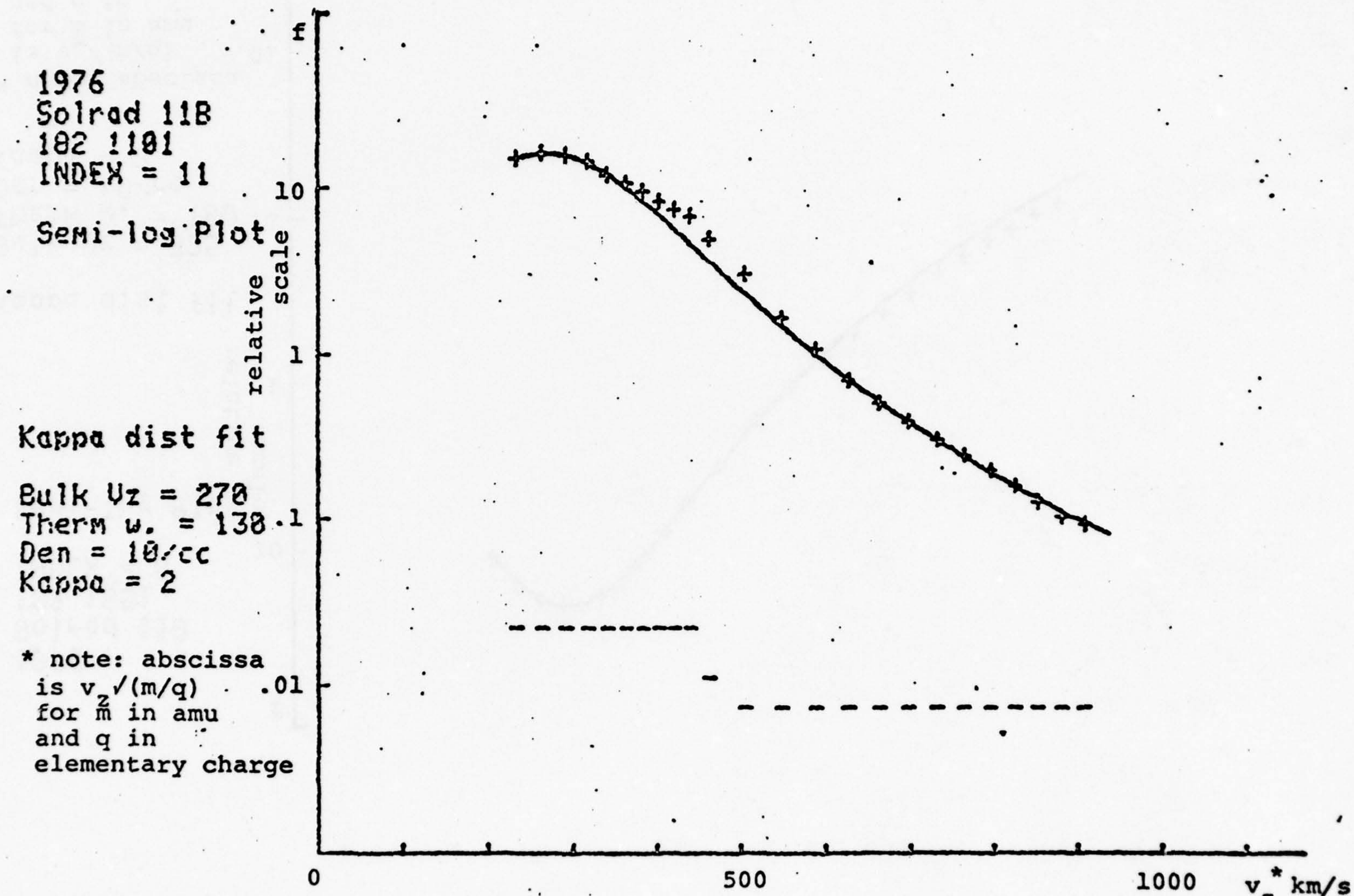

1976
Solrad 11B
182 1101
INDEX = 11
Semi-log Plot
Kappa dist fit
Bulk Vz = 270
Therm w. = 130
Den = 10/cc
Kappa = 2
* note: abscissa
is $v_z\sqrt{(m/q)}$
for m in amu
and q in
elementary charge
f
relative scale
10
1
.1
.01
0
500
1000
v_z^* km/s

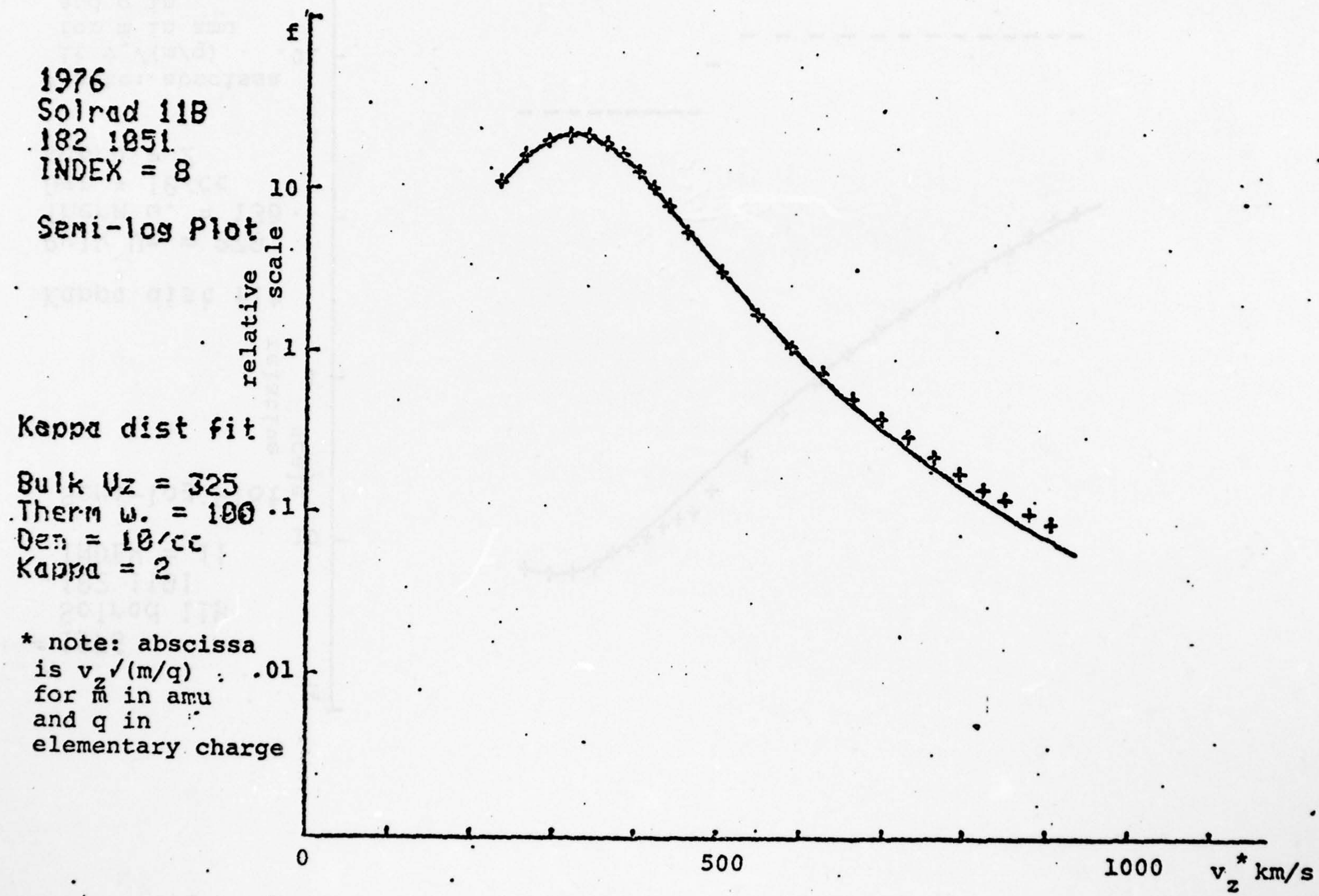
1976
Solrad 11B
182 1051
INDEX = 8
Semi-log Plot
Kappa dist fit
Bulk Vz = 325
Therm w. = 100
Den = 10/cc
Kappa = 2
* note: abscissa
is $v_z \sqrt{(m/q)}$
for m in amu
and q in
elementary charge
f
relative scale
10
1
.1
.01
0
500
1000
v_z^* km/s

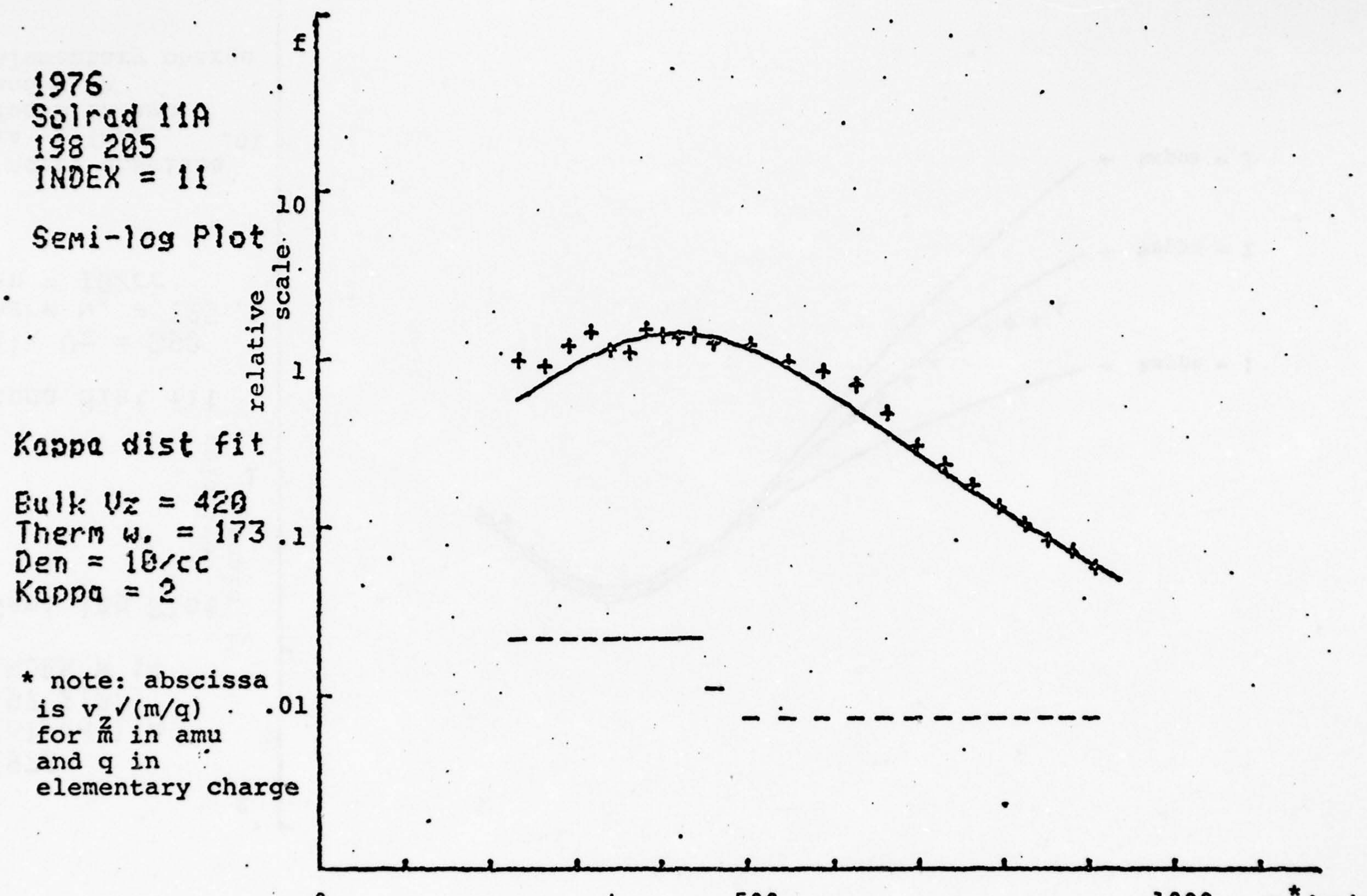

Magnetosheath spectrum which is found near the magnetopause

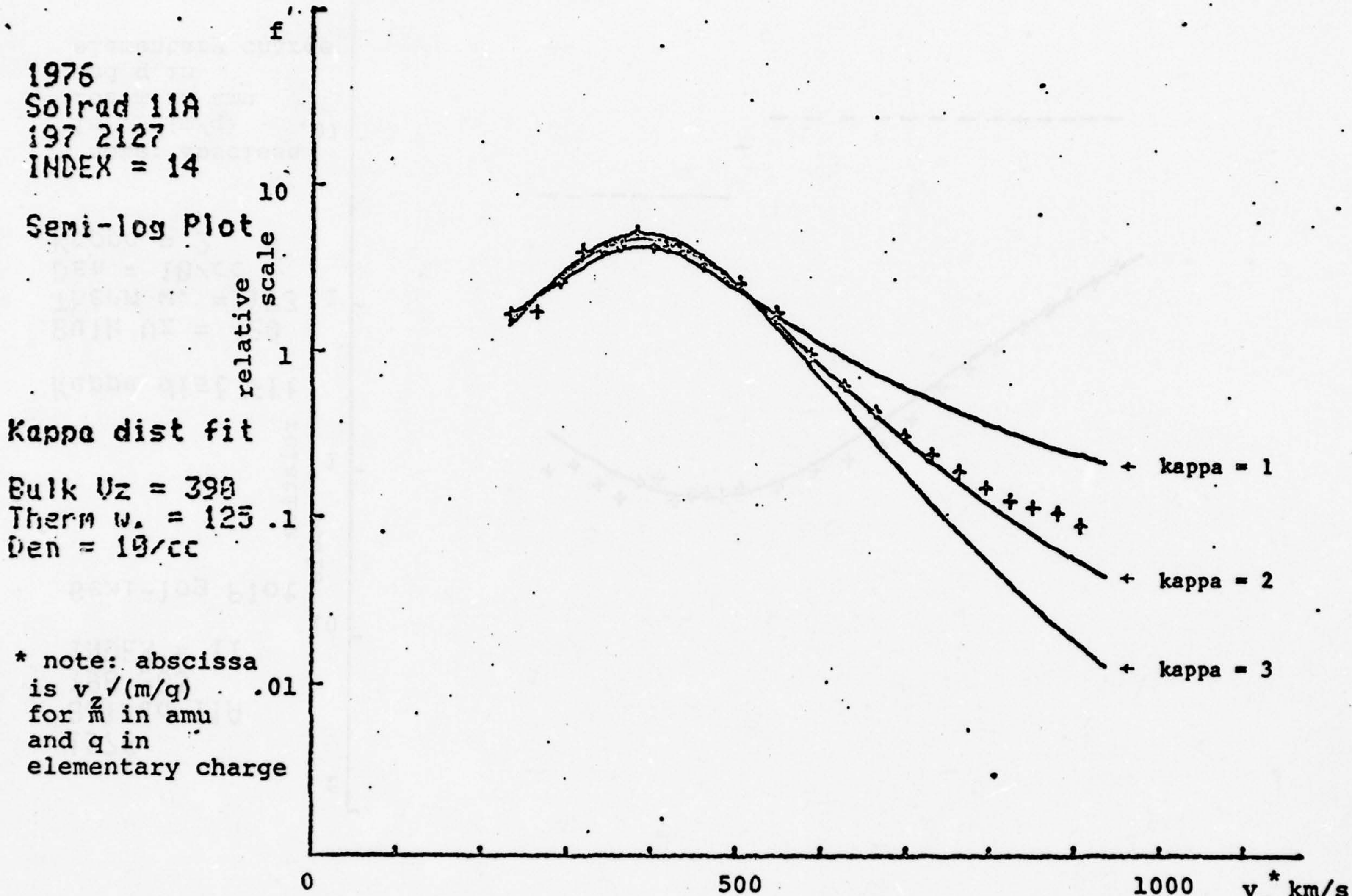

Spectrum of magnetosheath that seems to have kappa less than 2

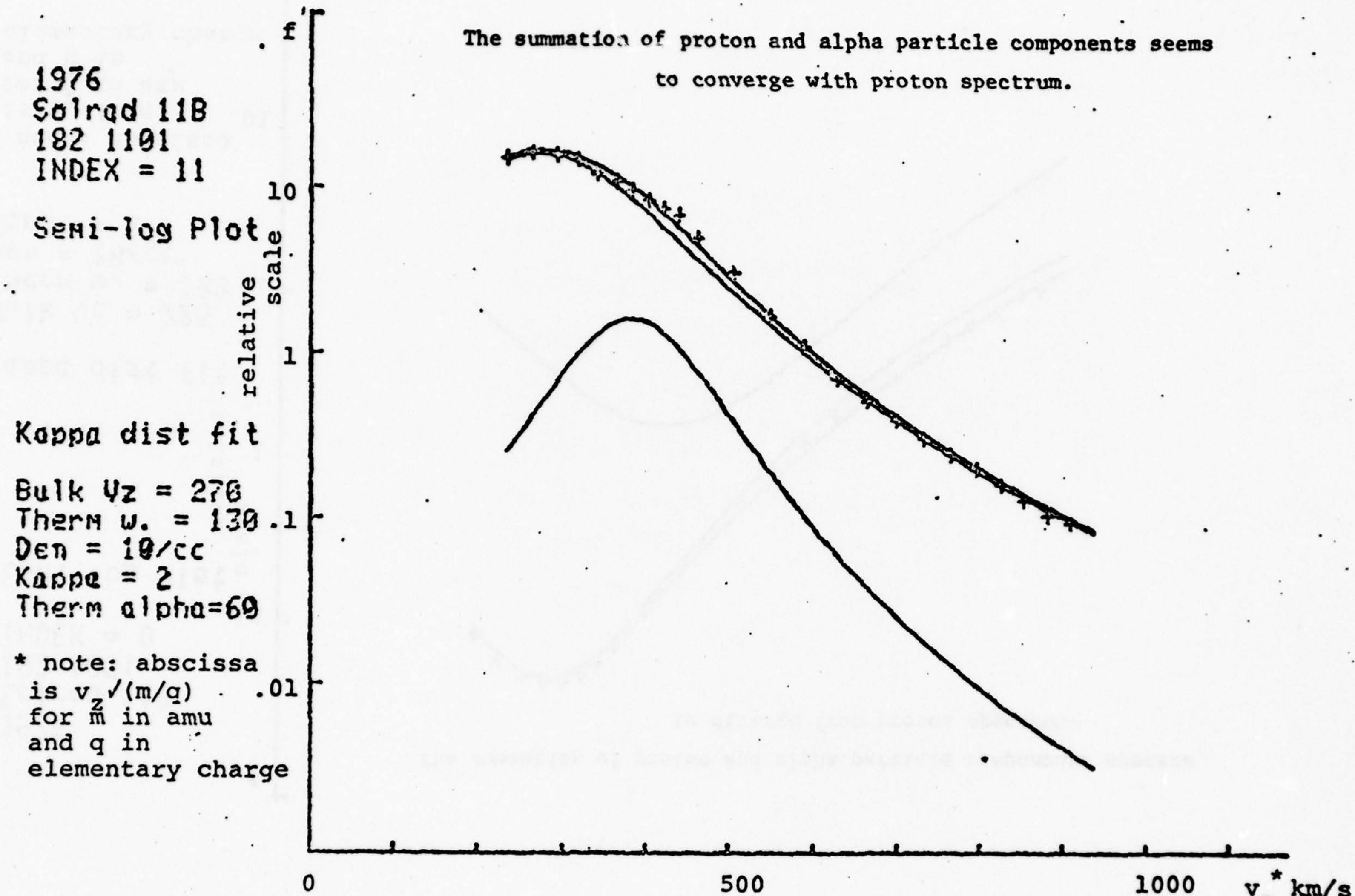
1976
Solrad 11B
182 1101
INDEX = 11
Semi-log Plot
Kappa dist fit
Bulk Vz = 270
Therm w. = 130
Den = 10/cc
Kappe = 2
Therm alpha=60
* note: abscissa
is $v_z\sqrt{(m/q)}$
for m in amu
and q in
elementary charge
f
relative scale
10
1
.1
.01
0
500
1000
v_z^* km/s
The summation of proton and alpha particle components seems
to converge with proton spectrum.

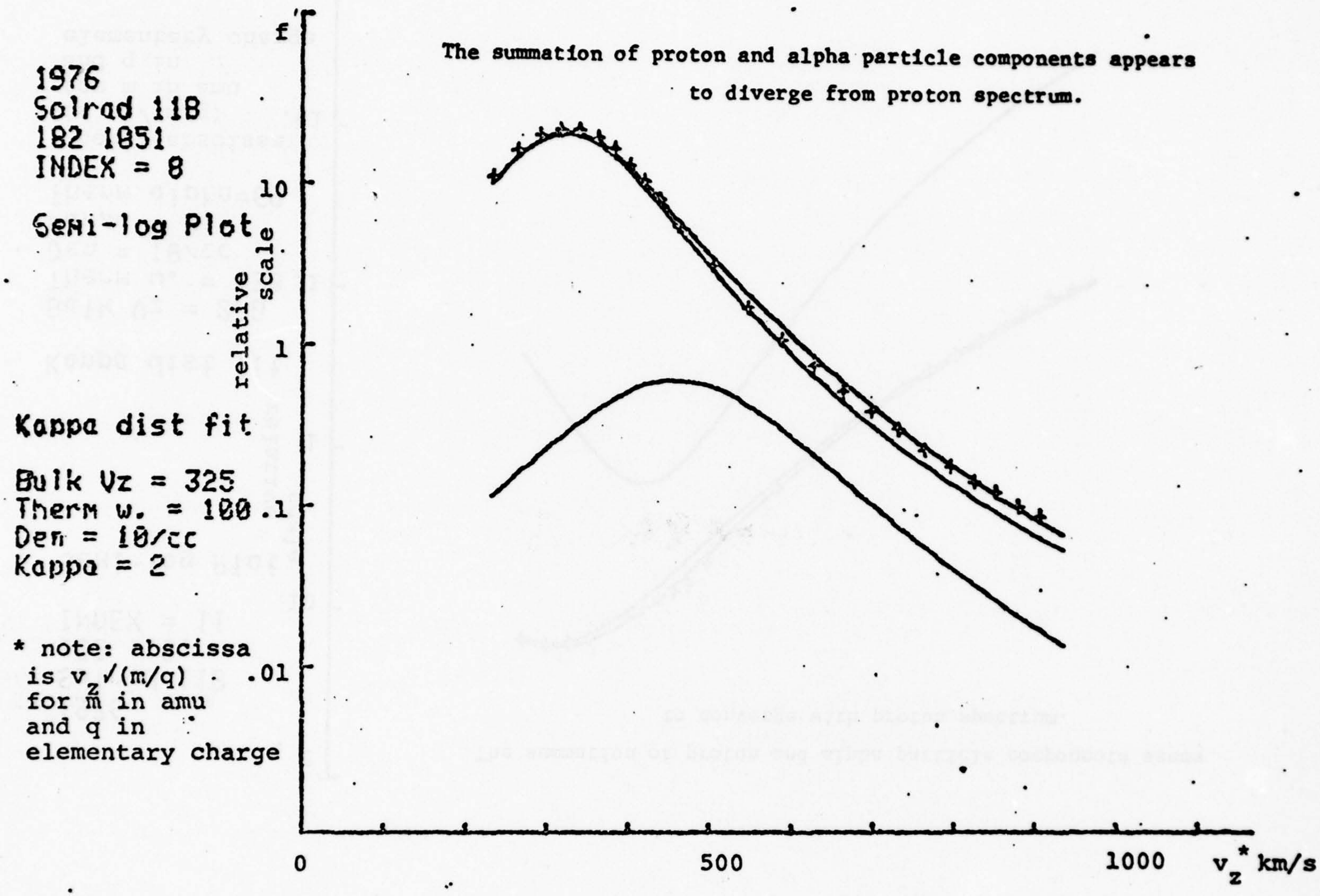
1976
Solrad 11B
182 1851
INDEX = 8
Semi-log Plot
Kappa dist fit
Bulk Vz = 325
Therm w. = 100
Den = 10/cc
Kappa = 2
* note: abscissa is $v_z\sqrt{(m/q)}$ for m in amu and q in elementary charge
f
relative scale
10
1
.1
.01
0
500
1000
v_z^* km/s
The summation of proton and alpha particle components appears to diverge from proton spectrum.

APPENDIX A

SOLRAD 'CURRENTS' PROGRAM

The beginning lines of the program set the values of constants.

```
 DIMENSION CURR(26)
 INTEGER*2 DN(26)
 INTEGER*2 DAY,HOUR
 REAL*4 NBULK,NTHERM
 DIMENSION AREA(10001)
 DIMENSION VOLTLO(32), VOLTHI(32)
 DATA VOLTLO /0.0,240.8,319.7,398.7,473.6,549.9,630.0,705.1,781.7,8
161.5,938.2,1015.5,1171.3,1405.3,1640.7,1878.0,2115.5,2351.7,2591.1
2,2831.3,3072.8,3314.4,3556.4,3800.6,4045.0,240.5/
 DATA VOLTHI /0.0,319.3,398.6,476.8,551.6,627.2,707.8,783.1,859.5,9
139.7,1016.1,1171.7,1406.1,1639.7,1875.1,2111.2,2348.4,2587.0,2826.
20,3067.3,3305.2,3548.3,3789.2,4033.1,4278.7,4279.5/
 DIMENSION XL(24),WL(24),XH(12),WH(12)
 DATA XL/-0.981560634,-0.904117256,-0.769902674,-0.587317954,
1        -0.367831499,-0.125233409,+0.125233409,+0.367831499,
2        +0.587317954,+0.769902674,+0.904117256,+0.981560634,
3        -0.981560634,-0.904117256,-0.769902674,-0.587317954,
4        -0.367831499,-0.125233409,+0.125233409,+0.367831499,
5        +0.587317954,+0.769902674,+0.904117256,+0.981560634/
 DATA WL/0.047175336,0.106939326,0.160078329,0.203167427,
1        0.233492537,0.249147046,0.249147046,0.233492537,
2        0.203167427,0.160078329,0.106939326,0.047175336,
3        0.047175336,0.106939326,0.160078329,0.203167427,
4        0.233492537,0.249147046,0.249147046,0.233492537,
5        0.203167427,0.160078329,0.106939326,0.047175336/
 DATA XH/-3.88972490,-3.02063703,-2.27950708,-1.59768264,
1        -0.947788391,-0.314240376,+0.314240376,+0.947788391,
2        +1.59768264,+2.27950708,+3.02063703,+3.88972490/
 DATA WH/2.65855168E-7,8.57368704E-5,3.90539058E-3,5.16079856E-2,
1        2.60492310E-1,5.70135236E-1,5.70135236E-1,2.60492310E-1,
2        5.16079856E-2,3.90539058E-3,8.57368704E-5,2.65855168E-7/
 DIMENSION VX(12),QT1SQ(12),XSQ(12)
 DATA RC,RA /2.750,1.50/
 DATA C1,C2 /6.94E-13,1.0367/
```

The following variables are inputs to the 'Currents' program:

DAY,HOUR = time spectrum taken

NBULK = bulk velocity in km/sec

NTHERM = the most probable thermal velocity in km/sec

DEN = the density of the plasma

BETA = shown below in degrees

ALFA = shown below set equal to zero in this present version original α,β representation:

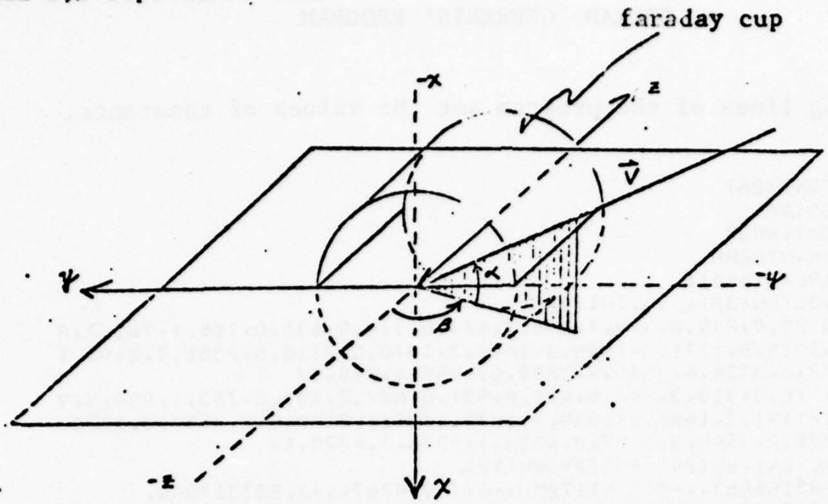

α =∠ subtended by v and its projection onto the yz plane

β =∠ subtended by -z axis and projection of v onto yz plane

CURR(26) is array listing current values in channels 1 to 26 calculated by the program

DN(26) is array listing datanumbers calculated after each CURR array is calculated

AREA(10001) stores the function relating overlapping area of solar wind image and collector plate to the linear displacement of their centers

VOLTLO(32), VOLTHI(32) VOLTLO(NCHAN) and VOLTHI(NCHAN) are respectively lower and upper voltage limits of the square wave grid modulation in the NCHAN channel

XL(24),WL(24),XH(12),WH(12) are sets of constants used in the numerical integrations

VX(12),QTISQ(12) store intermediate values in the integration

RC=2.75 inches= radius of collector plate

RA=1.5 inches= aperture radius

```
      IVERS 7132
      LOGICAL*4 FW(5)
      CALL HACK(FW)
      WRITE (6,1020) FW(1),FW(2),IVERS
 1020 FORMAT(69H1CURRENT ON THE FULL COLLECTOR PLATE USING AN EXACT AREA
     1 CALCULATION. ,T111,2A4/27H SOLRAD.   ENERGY CHANNELS ,T111,
     28HVERSION I4)
      ICOUNT = 0
      DO 1 I = 1,29
    1 CURR(I) = 0.0
```

IVERS = date of revision of program = 7132 = day 132 in 1977

HACK subroutine at LNS computation facility returns the date the job is run

CURR array set to zero

the following values are used for AREA(10001) determination:

```
      PI=3.1415927
      ANORM=PI*RA*RA
      TRC=2.*RC
      TRA=2.*RA
      RCSQ=RC*RC
      RASQ=RA*RA
      BND1=(RC-RA)**2
      BND2=RC*RC-RA*RA
      BND3=(RC+RA)**2
      HPSRSQ=0.5*PI*(RCSQ+RASQ)
      VBAR = -110.
      Q=1.6021E-19
      REM=1.67252E-27
      AN=10E5*Q
```

ANORM is aperture area
VBAR = -110. is suppressor grid voltage in volts

Q= 1.602×10^{-19} is elementary charge in coulombs

REM = 1.67252×10^{-27} is proton rest mass in kg

AN = $10^6 \times Q$ = value used in normalization

<u>Determination of function represented by AREA(10001)</u>

The area of overlap, A, shaded in the following diagram, is determined as a function of U, the displacement between the centers of the circles

A = area in sector ADC + area in sector BDC - area in ADBC

$$A = \left(\frac{2a}{2\pi}\right)\pi(RC)^2 + \left(\frac{2b}{2\pi}\right)\pi(RA)^2 - 2(\tfrac{1}{2}xU)$$

$$A = a(RC)^2 + b(RA)^2 - xU$$

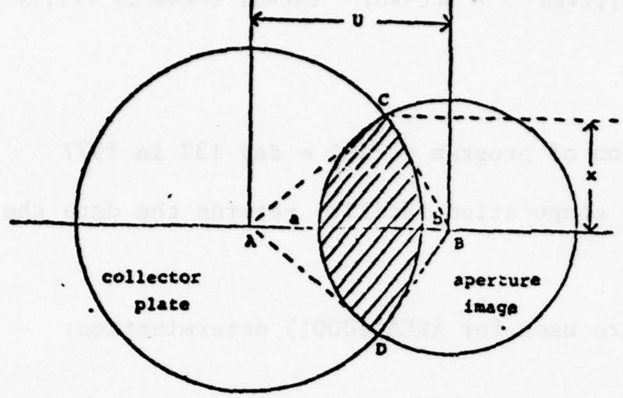

$x = (RC)\sin a = (RA)\sin b$

$$\cos a = \frac{U^2+RC^2-RA^2}{2U(RC)} \qquad \cos b = \frac{U^2+RA^2-RC^2}{2U(RA)}$$

$$\left.\begin{aligned} ARG1 &= \cos a = (U^2+BND2)/(TRC\cdot U) \\ ARG2 &= \cos b = (U^2-BND2)/(TRA\cdot U) \end{aligned}\right\} \text{ from defined terms}$$

from * above:

$$A = \cos^{-1}\left(\frac{U^2+RC^2-RA^2}{2U\cdot RC}\right)RC^2 + \cos^{-1}\left(\frac{U^2+RA^2-RC^2}{2U\cdot RA}\right)RA^2 - RA\sin(\cos$$

$$- RA\sin\left(\cos^{-1}\left(\frac{U^2+RA^2-RC^2}{2U\cdot RC}\right)\right)U$$

Therefore:

$$A = RC^2\cos^{-1}(ARG1) + RA^2\cos^{-1}(ARG2) - U(RA)\sin(\cos^{-1}(ARG1))$$

This equation is used in the following DO LOOP:

```
      VELPRO=2.*Q/REM
C *** CALCULATE AREA OVERLAP AS FUNCTION OF DISPLACEMENT OF CENTERS OF
C     COLLECTOR AND PROJECTION OF APERTURE ONTO COLLECTOR
      DO 5 I=2,10000
      U=2.*RA*FLOAT(I-1)/10000.+RC-RA
      USQ=U*U
      ARG1=(USQ+BND2)/(TRC*U)
      ARG2=(USQ-BND2)/(TRA*U)
      AREA(I)=HPSRSQ-RCSQ*ARSIN(ARG1)-RASQ*ARSIN(ARG2)-U*RA*SQRT((1.-ARG
     12)*(1.+ARG2))
    5 CONTINUE
      AREA(1)=ANORM
      AREA(10001)=0.0
      SLOPE=10000./TRA
      BI=10000.*(RA-RC)/TRA+1.5
C ****DIMENSIONS OF METERS, KILOGRAMS, AND SECONDS - EXCEPT FOR CUP
C     WHICH IS IN INCHES
C *** DEN IS DENSITY PER CC
      ALF=0
```

The index I specifies 10001 values of U in constant increments from (RC-RA) to (RC-RA) and the area is calculated for each I.

This enables addressing of AREA to get a sufficient approximation to the area of overlap at specific abscissas in the integration.

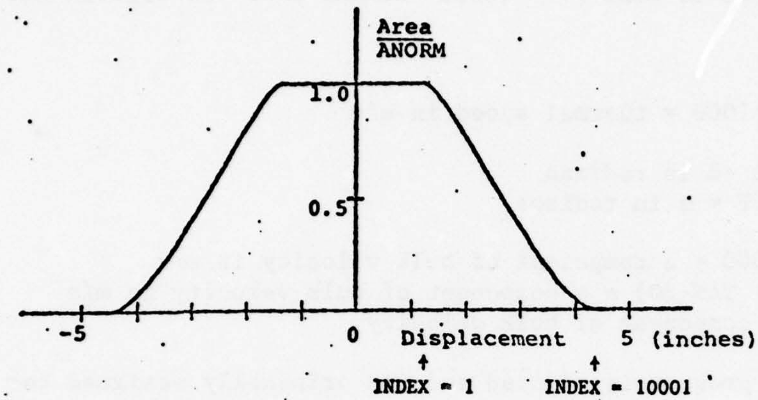

Determining INDEX from U:

INDEX = SLOPE·U + B1 for SLOPE and B1 given

since we let $\text{INDEX} = \dfrac{10000(U+RA-RC)}{2RA} + 1.5$.

The value of 1 becomes 1.5 so that one obtains the closest approximation to the fixed variable INDEX from the floating terms.

```
      ALFA=ALF*0.01745329
   7  READ(5,1200,END=7777)DAY,HOUR,NBULK,DEN,NTHERM,BE
1200  FORMAT(I3,I5,F7.1,3F5.1)
   8  ICOUNT = ICOUNT+1
      IF  (ICOUNT,EQ.64.OR.ICOUNT.EQ.128) GO TO 8
C *** NBULK= RADIAL VELOCITY=Z-COMPONENT IN KM/SEC
      THERM = NTHERM*1000
      BETA = BE
      BO=BETA*0.01745329
      COSAL=COS(ALFA)
      BULKVZ= NBULK*1000
      BULKVY= BULKVZ*TAN(BO)
      BULKVX= 0
      ALPHA=THERM**(-2)
      DO 15 I = 1,12
      VX(I)=XH(()*THERM+BULKVX
  15  CONTINUE
```

ICOUNT = an index thatnumbers the spectra

If ICOUNT = 64 or 128 the values are not used since these values and 0 specify the calibration modes

At the end of inputting all cards with parameter data at line 7 control is transferred to line 7777 where 'NORMAL EXIT' is written and the program stops.

THERM = NTHERM·1000 = thermal speed in m/s

BO = .0174 BETA = β in radians
ALFA = .0174 ALF = α in radians

BULKVZ = NBULK·1000 = z component of bulk velocity in m/s
BULKVY = BULKVZ · TAN(BO) = y component of bulk velocity in m/s
BULKVZ = 0. = x component of bulk velocity

The 'Currents' program is adapted and was originally designed for a three-dimensional problem. It can be essentially reduced to a two-dimensional integration. By setting α to zero, our problem is a two-dimensional one with the value for β corresponding to the value of THETA in the Solrad 'Analysis' Program where the angle is computed.

The following diagram shows the velocity components for non-zero α:

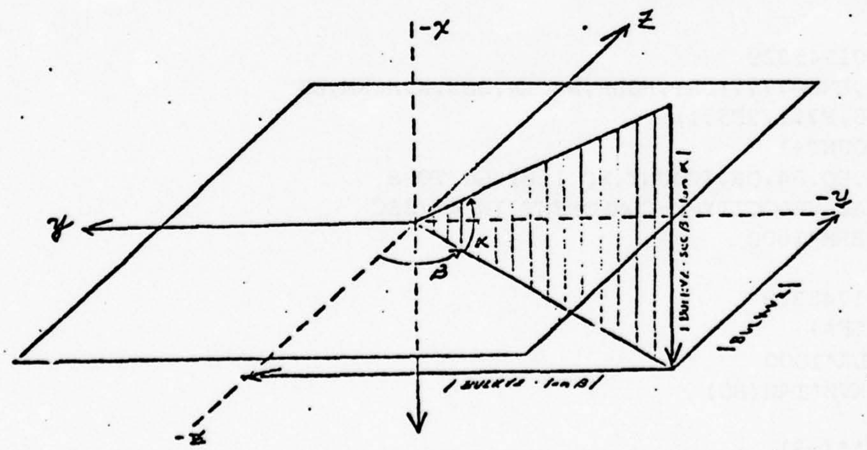

VX(I) = XH(I) * THERM + BULKVX are the x-components of velocity used in the Hermite numerical integration method described in page 56.

```
      CONST = (6.45E-4)*0.735*AN*(ALPHA/PI)**(1.5)*DEN
C *** VBOT AND VTOP ARE LIMITS OF INTEGRATION AS SET BY THE DISTRIBUTION
C    FUNCTION
      VBOT=BULKVZ-3.5*THERM
      VTOP=BULKVZ+3.5*THERM
      NCHAN = 2
      CURMAX=0.0
   77 CONTINUE
C *** VLGRID AND VHGRID ARE LIMITS OF INTEGRATION AS SET BY THE VOLTAGES ON
C    THE GRIDS
      VLOW=VOLTLO(NCHAN)
      VHI=VOLTHI(NCHAN)
      VLGRID = SQRT(VELPRO*VLOW)
      VHGRID = SQRT(VELPRO*VHI)
      IF (VLGRID.GE.VTOP) GO TO 170
      IL=1
      IH=24
      VZ1L = AMAX1(VLGRID,VBOT)
      VZ1H = AMIN1(VHGRID,VTOP)
      IF(VBOT.LE.VHGRID) GO TO 17
      IL = 13
      VZ1H = VBOT
```

$CONST = (6.45 \times 10^{-4})(.735)AN(\gamma)\pi^{-3/2}DEN$ for γ = ALPHA
is used immediately after the triple integration

(6.45×10^{-4}) converts sq.in. used in AREA to m^2.
.735 = transparency, the fraction allowed through grids
AN = $10^6 Q$ which converts density units from #/cc to #/m^3

$\gamma\pi^{-3/2} = (\gamma/\pi)^{3/2}\gamma^{1/2}$ = distribution function normalization times constant used in Hermite integration

DEN = density of plasma in #/cc

VBOT = BULKVZ - 3.5 * THERM   VTOP = BULKVZ - 3.5 * THERM

The v_z integration involves Gaussian Integration and limits are therefore needed for the distribution function. With these limits, the fractional deviation from the exact value is -7.4×10^{-7}, within the accuracy of the integration method.

VHI and VLOW become the upper and lower voltage limits in the grid modulation.

VLGRID = (VELPRO·VLOW) = $(2Q \cdot VLOW/m_p)$
VHGRID = (VELPRO·VHI) = $(2Q \cdot VHI/m_p)$

These are the velocity limits corresponding to the voltage limits. This is from $QV = \frac{1}{2} m_p v_z^2$, the relation between V and proton velocity limit.

If VLGRID $\leq$ VTOP at line 170 SUMLO = SUMHI = 0.0 so CURR(NCHAN) = 0. in output since too few protons exist in distribution function above VLGRID.

The z-integration is divided into two parts to take into account a second effect producing a pulsated component of current (CURR(NCHAN)). Both of the following contribute to the value of CURR(NCHAN):

(1) The difference in number of protons admitted through at grid voltage VHI and VLOW.

(2) The difference in area of interception of plasma image with the collector plate at VHI and VLOW due to the refraction by the grid potential of protons entering at an angle to the cup's axis.

(1) is given by the integral of the distribution function between VLGRID and VHGRID and this integration is indexed by $1 \leq I \leq 12$. Integration of (2) is indexed by $13 \leq I \leq 24$ and involves integrating over all velocities above VLGRID.

VZIL = maximum of (VLGRID,VBOT) = lower limit for integration (1)

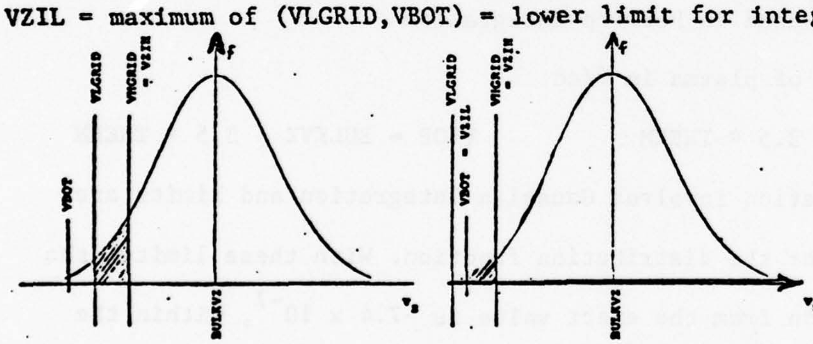

That is, no integration is done below VBOT or VLGRID. Similarly with VZIH = minimum of (VHGRID,VTOP), no integration is done above VHGRID <u>and</u> VTOP.

If VBOT>VGRID we see that IL = 1 and IH = 24 meaning that I would vary from 1 to 24 performing both integrations. If VBOT VHGRID integration (1) is unnecessary due to a low distribution value and IL=13 and IH=24 so that integration (2) is performed with the lower limit equalling VBOT.

Constants used in integration

(1)

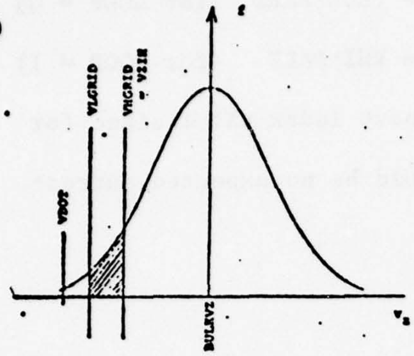

(2)

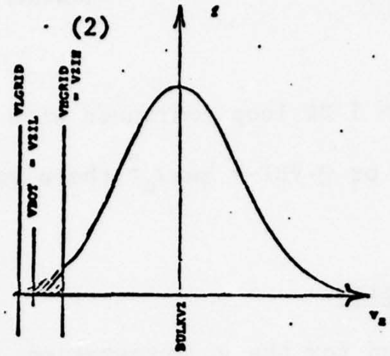

AVABL and AVABH are midpoints in the region of interest, AVBEL and AVBEH respectively half of the range in each. They therefore have the values shown in the program.

To accomplish the triple integration, there is a nest of three DO loops, the outermost loop doing the v_z integration, begins at the DO 120 statement.

```
17 AVBEL = 0.5*(VZ1H-VZ1L)
   AVABL=0.5*(VZ1H+VZ1L)
   AVBEH=0.5*(VTOP-VZ1H)
   AVABH=0.5*(VTOP+VZ1H)
   LOOP=0
20 VALUE=0.0
   DO 120 I=IL,IH
   IF(I.GE.13)GO TO 22
   VZ=AVBEL*XL(I)+AVABL
   AVBE=AVBEL
   GO TO 24
22 VZ=AVBEH*XL(I)+AVABH
   AVBE=AVBEH
24 VZINV=1./VZ
   PART=Q*2./(REM*VZ**2)
   VLPART=VLOW*PART
   IF(LOOP.EQ.1)VLPART=VHI*PART
   IF(VLPART.GT.1.)GO TO 120
   B = 2.55/(1.+SQRT(1.-VLPART)) + 1.22/(1.+SQRT(1.-VBAR*PART))+1.02
```

B is the term used to determine displacement due to refraction as shown on page 56. Variable LOOP has value 0 or 1. Integration is done once for each value. The integrations are identical except that LOOP = 0 determines refraction for modulator grid voltage = VLOW and LOOP = 1 determines refraction for modulator grid voltage = VHI.

$\text{PART} = Q/(\frac{1}{2}m_p v_z^{\,2})$ $\quad\quad$ $\text{VLPART} = \text{VLOW}\cdot\text{PART}$ (for LOOP = 0)

$= \text{VHI}\cdot\text{PART}$ (for LOOP = 1)

If VLPART > 1 DO loop continued with next index value since for $Q\cdot\text{VLOW} > \frac{1}{2}m_p v_z^{\,2}$ or $Q\cdot\text{VHI} > \frac{1}{2}m_p v_z^{\,2}$ there would be no expected current.

Hermite Integration

This is used for the v_x integration.

$$\int_{-\infty}^{\infty} e^{-x^2} f(x)dx \approx \sum_{k=1}^{12} \omega_k f(x_k)$$

where x_k are the zeroes of the Hermite polynomial for n = 12. ω_k are weight factors. The array elements XH(K) equal x_k and WH(K) equals ω_k. The innermost integral is of the form

$$\int_{-\infty}^{\infty} e^{-\gamma(v_x-v_x')^2} \text{AREA}(v_x',v_y',v_z')dv_x'$$

for v_x = BULKVX. Therefore we let $x = \gamma^{\frac{1}{2}} v_x = (v_x - v_x')/\text{THERM}$. Then $dv_x' = \gamma^{-\frac{1}{2}}dx$, this constant appearing in the constant term in page 52. x_k = XH(I) = -(BULKVX-VX(I))/THERM for VX(I) = v_x' = integration variable. Finally,

VX(I) = XH(I)*THERM + BULKVX

are the x-components of the velocity used in the integration as in page 51.

Gaussian Integration

This is used for v_z and v_y integration.

$$\int_{-1}^{1} f(x)dx \approx \sum_{k=1}^{12} \omega_i f(x_i)$$

for x_i the zeroes of Legendre polynomial for n=12. We want to evaluate functions of the form $\int_{v1}^{v2} f(v)dv$ where

$$\int_{v1}^{v2} f(v)dv = \int_{v1-(v1+v2)/2}^{v2-(v1+v2)/2} f(v+(v1+v2)/2)dv = \int_{-(v2-v1)/2}^{(v2-v1)/2} f(v+(v1+v2)/2)dv \;.$$

Let x = (v/((v2-v1)/2). Then $\int_{v1}^{v2} f(v)dv =$

$$\frac{v2-v1}{2}\int_{-1}^{1} f(x)dx = \tfrac{1}{2}(v2-v1)\sum_{i=1}^{12} \omega_i f(x_i).$$

This explains the derivation of integration constants on page 54 .

Calculation of refraction

The refraction of one ion as it passes through the grids causes it to traverse a horizontal distance l that is a function of tangential velocity and the time of traversal.

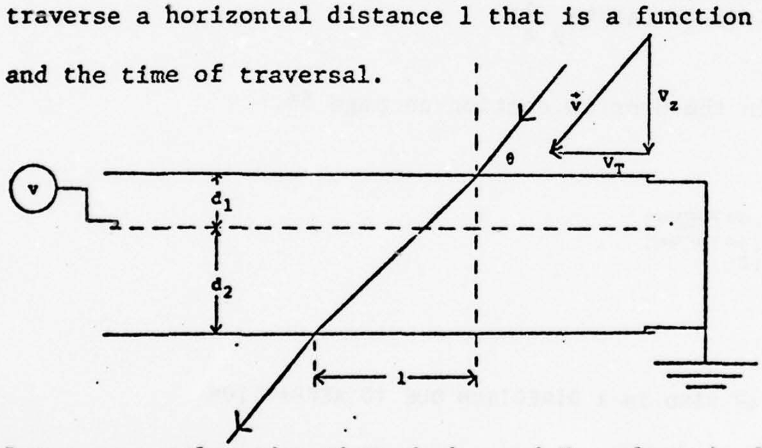

$D = d_1 + d_2$

V = grid voltage

Let a_1 = acceleration through d_1, and E = electric field.

$$a_1 = \frac{QE}{m_p} = \frac{QV}{m_p d_1} \qquad d_1 = v_z t_1 + \frac{a_1 t_1^{\,2}}{2}$$

Let $v_T = \sqrt{(v_x^2 + v_y^2)}$ = initial tangential proton velocity. Then

$$t_1 = \frac{-v_z \pm \sqrt{(v_z^2 - \frac{2QV}{m_p})}}{-QV/m_p d_1} = \frac{m_p d_1 v_z}{QV}\left(1 \pm \sqrt{(1 - \frac{QV}{\frac{1}{2} m_p v_z^2})}\right)$$

Because of time-reversal symmetry, for t_2 the time to traverse d_2,

$$t_2 = \frac{m_p d_2 v_z}{QV}\,(1 \pm \sqrt{(1 - QV/(\tfrac{1}{2}m_p v_z^2))}).$$

Therefore, the total time, t, is

$$t = t_1 + t_2 = \frac{mv_z D}{QV}\,(1 - \sqrt{(1 - QV/(\tfrac{1}{2}m_p v_z^2))}).$$

The sign is negative so that $t = D/v_z$ for $V = 0$. Therefore,

$$l = v_T t = v_T \frac{mv_z D(1 - \sqrt{(1 - QV/\tfrac{1}{2}m_p v_z^2)}}{QV(1 + \sqrt{(1 - QV/\tfrac{1}{2}mv_z^2)}} = \frac{v_T}{v_z}\left(\frac{2D}{1 + (1 - QV/\tfrac{1}{2}m_p v_z^2)}\right)$$

Let $B = \dfrac{2D}{1 + \sqrt{(1 - QV/\tfrac{1}{2}m_p v_z^2)}} + \dfrac{2D_s}{1 - \sqrt{(1 - Q \cdot VBAR/\tfrac{1}{2}m_p v_z^2)}} + 1.02$

Then $l = \dfrac{v_T}{v_z} B$. B is shown in the program section on page 54.

```
      BOT = -VZ*(RA+RC)/B
      TOP=-BOT
      ALIM=AMAX1(BOT,BULKVY-2.5*THERM)
      BLIM=AMIN1(TOP,BULKVY+2.5*THERM)
      IF(BLIM.LE.ALIM) GO TO 185
      AVBE1=0.5*(BLIM-ALIM)
      AVAB1=0.5*(BLIM+ALIM)
      DO 25 L=1,12
      QT1=VX(L)*VZINV
      QT1SQ(L)=QT1*QT1
C *** X = DISPLACEMENT OF SOLAR WIND IN X DIRECTION DUE TO REFRACTION
C     FROM CHARGED GRIDS
      X=B*QT1
      XSQ(L)=X*X
   25 CONTINUE
      ZPART=ALPHA*(VZ-BULKVZ)**2
      IF(ZPART.GE.70.)ZPART=70.
      PHIZ=VZ*EXP(-ZPART)
      VALUE1=0.0
```

The maximum l that can produce a current on the plate is l=(RA+RC). The velocity corresponding to this displacement has the value BOT for the transverse component (v_T). Since RA + RC = $\left(\dfrac{-BOT}{v_z}\right)B$, BOT = $-v_z \cdot$(RA + RC)/B.

v_y integration limits

Therefore, v_y needn't be integrated for v_y < BOT or v_y < -BOT. Let TOP = -BOT. Thus ALIM and BLIM are limits of integration for v_y since the value of the distribution function is too low outside of

$$(\text{BULKVY}-2.5\text{THERM} \le v_y \le \text{BULKVY}+2.5\text{THERM})$$

which encloses all but 4×10^{-4} of the area.

ALIM = maximum of (BOT,BULKVY - 2.5THERM)
BLIM = minimum of (TOP,BULKVY + 2.5THERM) .

Let A=BULKVY-2.5 THERM and B=BULKVY+2.5 THERM. Possible situations are depicted as follows:

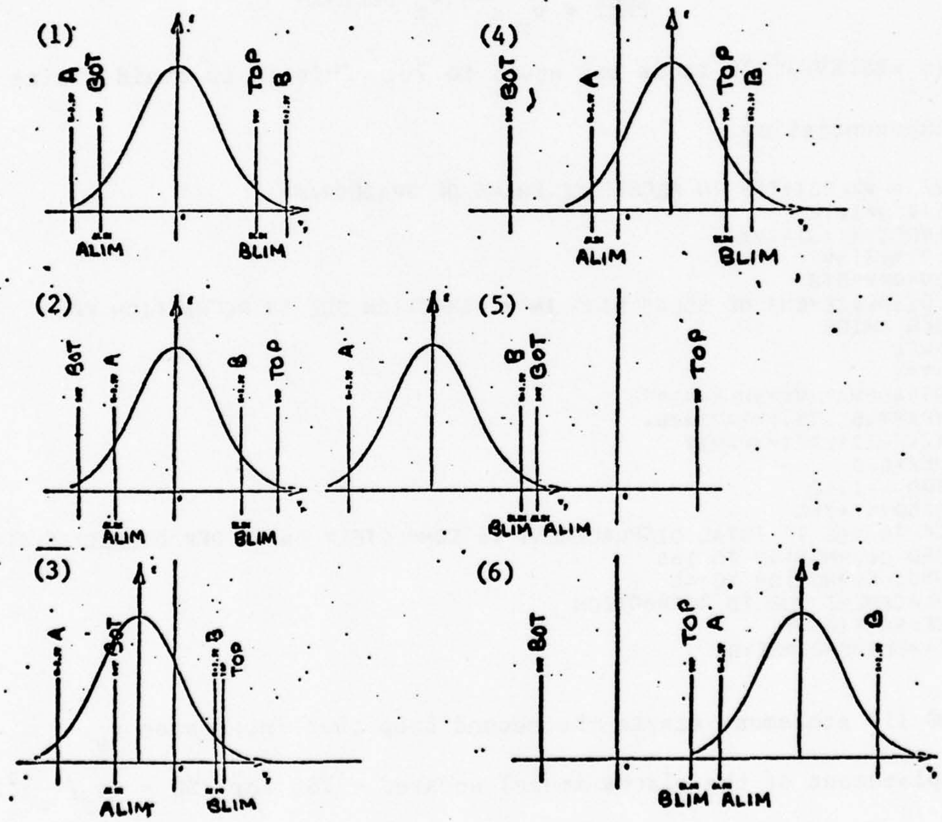

Only cases (5) and (6) should be avoided, which is accomplished by IF(BLIM.LE.ALIM) GO TO 185 which writes the values of ALIM and BLIM and sets CURR(NCHAN)=0., and proceeds with the program.

AVBE1 = .5(BLIM - ALIM)
AVAB1 = .5(BLIM + ALIM)

These constants of integration are,as explained for v_z, used with the Gaussian integration.

The DO 25 loop determines the plasma displacement in the x-direction at each abscissa (VX(L)) used in integration and places its square in array XSQ(L) :

$$XSQ(L) = \left(\frac{VX(L)}{v_z}\right)^2 B^2 \quad \text{since } VZINV = v_z^{-1} \text{ on page 54.}$$

<u>Function of v_z integrated</u>

$$PHIZ = v_z\, e^{-\gamma(v_z - BULKVZ)^2}$$

If $\gamma(v_z\text{-BULKVZ})^2 \geq 70$ it is set equal to 70. This is to avoid a size error in exponentiation.

```
C *** VY,VZ = VELOCITIES IN REFERENCE FRAME OF SPACECRAFT
      DO 110 J=1,12
      VY=AVBE1*XL(J)+AVAB1
      OT2=VY*VZINV
      OT2SQ=OT2*OT2
C *** Y = DISPLACEMENT OF SOLAR WIND IN Y DIRECTION DUE TO REFRACTION FROM
C     CHARGED GRIDS
      Y=B*OT2
      YSQ=Y*Y
      YPART=ALPHA*(VY-BULKVY)**2
      IF(YPART.GE.70.)YPART=70.
      PHIYZ=PHIZ*EXP(-YPART)
      VALUE2=0.0
      DO 100 K=1,12
      DSQ=XSQ(K)+YSQ
C *** CHECK TO SEE IF TOTAL DISPLACEMENT IS COMPLETELY ON OR OFF COLLECTOR PLATE
      IF(DSQ.GE.BND3)GO TO 100
      IF(DSQ.LE.BND1)GO TO 40
C *** DISPLACEMENT DUE TO REFRACTION
      DIPSE=SQRT(DSQ)
      INDEX=SLOPE*DIPSE+B1
```

The DO 110 statement starts the second loop that integrates v_y. The (y-displacement of the plasma image) squared = YSQ for YSQ = $(v_y/v_z)^2 B^2$ obtained in the same manner as XSQ(L).

The function integrated is obviously a function of v_z. It is

$$PHIYZ = e^{-\gamma(v_z - BULKVZ)^2} e^{-\gamma(v_y - BULKVY)^2}$$

$$PHIYZ = PHIZ\ e^{-\gamma(v_y - BULKVY)^2} = PHIZ\ e^{-YPART}$$

and numerical integration on v_y is performed for each value of PHIZ. As before, the maximum value of YPART is 70.

The v_x integration starts at the DO 100 statement each time the loop is entered with a different value for YSQ. Each value of XSQ is added to it with each index value of the loop.

DSQ = XSQ(K) + YSQ

Thus, the square of the total displacement is known for each value of v_x. The following cases for DSQ are considered:

I) DSQ $\geq$(RC + RA)^2

i.e. DSQ $\geq$ BND3

Loop is continued for next value of k since no current contribution to integral

II) DSQ $\leq$ (RC - RA)^2

i.e. DSQ $\leq$ BND1

INDEX = 1 for area determination

III) (RC - RA)^2 < DSQ < (RC + RA)^2

The AREA array is used

DIPSE = $\sqrt{}$(DSQ). Thus, since INDEX = SLOPE · DIPSE + B1 at each value of DIPSE to reference AREA value at each displacement.

The following section completes the triple integration.

```
      GO TO 90
   40 INDEX=1
   90 VALUE2 = VALUE2 + WH(K)*AREA(INDEX)
  100 CONTINUE
      VALUE1 = VALUE1 + WL(J)*PHIYZ*VALUE2
  110 CONTINUE
      VALUE=VALUE+WL(I)*AVBE1*AVBE*VALUE1
  120 CONTINUE
      VALUE=CONST*VALUE
      LOOP=LOOP+1
```

Statement 90 completes v_x integration since, as shown on page 55,

$$\int_{\infty}^{\infty} e^{-\gamma(v_x - v_x')} \text{AREA}(v_x', v_y', v_z')\, dv = \sum_{K=1}^{12} \omega_k \text{AREA}(\text{VX}(K), \text{VY}(J), \text{VZ}(I))$$

for ω_k = WH(K) and AREA function determined by INDEX. VALUE2 originally set at zero.

VALUE1 = VALUE + WL(J) · PHIYZ ·VALUE2

$$= \sum_{J=1}^{12} \left(\sum_{K=1}^{12} \text{WH}(K)\text{AREA}(\text{INDEX}) \right) e^{-\gamma(\text{VY}(J)-\text{BULKVY})^2} e^{-\gamma(v_z - v_z')^2} v_z$$

since VALUE = 0. originally.

VALUE = VALUE + WL(I) · AVBE1 · AVBE · VALUE1

$$= \sum_{I=IL}^{IW} \left(\sum_{J=1}^{12} \left(\sum_{K=1}^{12} \text{WH}(K)\text{AREA}(\text{VX}(K), \text{VY}(J), \text{VZ}(I)) \right) \right) e^{-\gamma(\text{VY}(I)-\text{BULKVY})^2} \cdot e^{-\gamma(\text{VZ}(I)-\text{BULKVZ})^2} \text{VZ}$$

which is the required equation.

To normalize, correct it dimensionally, and take into account transparency, and elementary charge:

VALUE = CONST · VALUE

for CONST = $(6.45 \times 10^{-4})(.735)(10^6)Q\gamma(\gamma\pi)^{-3/2}$ as described in page 52.

AVBE1 and AVBE are needed as shown in page 59.

```
      GO TO(125,130),LOOP
  125 SUMLO=VALUE
      IF (VHGRID.GE.VTOP) GO TO 180
      IL=13
      IH=24
      GO TO 20
  130 SUMHI=VALUE
  140 CURR(NCHAN) = SUMLO-SUMHI
      IF(CURR(NCHAN).LT.CURMAX) GO TO 47
      CURMAX=CURR(NCHAN)
   47 CONTINUE
      IF (NCHAN.EQ.26) GO TO 50
      IF(CURR(NCHAN).LT.CURMAX*.0001) GO TO 49
   48 NCHAN = NCHAN + 1
      GO TO 77
   49 MN=NCHAN+1
      DO 51 IJ=MN,25
   51 CURR(IJ)=0.0
      NCHAN=26
      GO TO 77
```

LOOP = LOOP + 1 changes LOOP = 0 to LOOP = 1 or LOOP = 1 to LOOP = 2 . Then, if LOOP = 1 goes to 125. For LOOP = 2 goes to 130 since both integrations are completed.

<u>LOOP = 1</u>

Integration (1) and (2) (page 53) just performed with VLPART = VLOW·PART from which the refraction is calculated for VLOW.

Thusly, integration (1) is finished since no particles enter grids with w velocity less than VZIH when grid voltage = VHI.

Integration (2) must be performed again to subtract DC current at voltage = VHI from DC current at VLOW to determine the modulation resulting from refraction.

If VHGRID VTOP there is no need to perform integration this second time since too few protons will enter with velocity greater than VZIH.

For second integration IL=13 and IH= 24 are lower and upper limits of the index. After these are set program goes to line 20 which starts v_z integration DO loop.

SUMLO = VALUE for LOOP = 1.

LOOP = 2

Integration performed with VLPART = VHI·PART. Then finally CURR(NCHAN) = SUMLO - SUMHI since we wish to subtract the results from each integration.

CURMAX has the value of the CURR(NCHAN) which is greatest for NCHAN from 2 to its present value.

If NCHAN = 26 then it goes to 50 where the last step of the program is to calculate the 26 data numbers. If not it goes to 77 and sets up the next integration.

If CURR(NCHAN) < .0001 CURMAX set all remaining CURR(NCHAN) to zero since all these currents will eventually correspond to the datanumber FF.

Control is transferred to statement 50 after all 26 CURR(NCHAN) are calculated.

The DO 57 loop determines the datanumbers, DN, for NCHAN = 2 to 26, the 24 contiguous positive ion channels and one large channel).

The DN array is printed first in decimal notation and secondly in hexadecimal notation. The input parameters are printed. Day, hour, and DN are punched on cards to enable the WIND2 program to make a check on this program.

```
C  *** CALCULATION FOLLOWS FOR DATA NUMBERS
   50 DN(1)=ICOUNT
      DU 57 I=2,26
      IF(CURR(I).LE.6.94E-13) GO TO 54
      DN(I)=255.0+ALOG*C1/CURR(I))/ALOG(C2)
      GO TO 57
   54 DN(I)=255
   57 CONTINUE
      WRITE(6,1070)DN
      WRITE(6,1007)DN
 1070 FORMAT(1HO,9X,I3,2X,24(I3,1X),1X,I3)
 1007 FORMAT(1H ,10X,Z2,3X,24(Z2,2X),1X,Z2)
      WRITE(6,1000)DAY,HOUR,NBULK,DEN,NTHERM,BETA
 1000 FORMAT(1H ,I3,1X,I5,4F6.1)
      WRITE(9,1025)DAY,HOUR,DN
 1025 FORMAT(I4,I4,1X,33Z2)
      GO TO 7
  185 WRITE(6,1080)BLIM,ALIM
 1C80 FORMAT(' BLIM LE ALIM  ',2E12.3)
  170 SUMLO=0.0
  180 SUMHI=0.0
      GO TO 140
 7777 WRITE(6.1050)
 1050 FORMAT(12HONORMAL EXIT)
      STOP
      END
```

APPENDIX B

LISTING OF MAXWELLIAN AND KAPPA FIT PROGRAM

```
1 GO TO 100
2 RETURN
4 PRINT K8(J);V7(J),W8(J),N1(J),H8(J,K0)
5 RETURN
8 PRINT "_ input kappa : ";
9 INPUT K8(J)
10 RETURN
12 PRINT "_ ht factor : ";
13 INPUT H8(J,K6)
14 RETURN
16 PRINT "_ LIST DATA FROM FILE # ";
17 INPUT N0
18 FIND N0
19 GO TO 85
20 K0=1
21 GO TO 2180
24 D8=1
25 RETURN
28 PRINT "_  input new scale : ";
29 INPUT S
30 RETURN
32 L0=2
33 GO TO 77
36 L0=0
37 RETURN
40 D7=0
41 GO TO 100
44 PRINT "_ input den : ";
45 INPUT N1(J)
46 RETURN
48 PRINT "_ input w. : ";
49 INPUT W8(J)
50 RETURN
52 PRINT "_ input bulk vz : ";
53 INPUT V7(J)
54 RETURN
56 GO TO 1010
60 K0=2
61 GO TO 2170
64 D8=0
65 RETURN
66 GO TO 430
68 S0=1
69 HOME
70 PRINT "nchan(0)=";
71 INPUT Z8
72 GO TO 540
73 GO TO 1540
76 GO TO 1540
77 D7=1
79 GO TO 480
80 D7=1
81 GO TO 480
82 GO TO 100
85 INPUT @33:M8,M9,M,M6,M7
86 PAGE
87 PRINT M;"
88 PRINT M6
89 PRINT M7
90 FOR I=1 TO 24
91 INPUT @33:M
92 PRINT "      ",M
93 NEXT I
94 FOR I=1 TO 11
95 INPUT @33:M
96 PRINT M
97 NEXT I
98 GO TO 90
100 PRINT "_ INPUT SPECTRUM HOUR : ";
```

```
110 INPUT M
120 J=0
130 J=J+1
140 IF L2(J)=M THEN 520
150 IF J<N7 THEN 130
160 PRINT "_ SPECTRUM NOT FOUND"
170 RETURN
180 DIM F(24,15),V7(15),N0(15),K8(15),H8(15,2),N1(15),A0(15)
190 DIM V(24),L1(16),L2(16)
200 N0=1
210 FOR K=1 TO 24
220 READ V(K)
230 NEXT K
240 DATA 0.167,0.189,0.209,0.227,0.243,0.259,0.273,0.287
250 DATA 0.3,0.313,0.33,0.359,0.39,0.419,0.447,0.473
260 DATA 0.497,0.52,0.543,0.565,0.586,0.606,0.626,0.645
270 FOR I=1 TO 15
280 V7(I)=0
290 NEXT I
300 D8=0
310 N7=0
320 S=1
330 S0=0
340 L0=1
350 DELETE 1,1
360 PAGE
370 WINDOW 0,25,0,30
380 VIEWPORT 30,130,20,100
390 PAGE
400 PRINT "G READY __    DATA COMPARISON PROGRAM__      G"
410 RETURN
420 K=0
430 K=K+1
440 IF K>N7 THEN 470
450 IF K>N6 THEN 470
460 IF N2(K)<>L2(J) THEN 430
470 GO TO 630
480 PRINT "_ INPUT SPECTRUM INDEX : ";
490 INPUT J
500 PAGE
510 D7=1
520 PAGE
530 GO TO 580
540 W2=(1403.7*V(Z8)-B)↑2/A↑2
550 F1=((1+1/C)/(1+W2/C))↑C*10↑D
560 U9=F(Z8,J)-F1
570 D7=1
580 VIEWPORT 30,130,20,100
590 IF L0=0 THEN 620
600 AXIS 2.137,6
610 GO TO 630
620 AXIS 2.137,0
630 N1=1
640 FOR I=1 TO 24
650 IF L0=2 THEN 680
660 X=30*V(I)
670 GO TO 690
680 X=20*LGT(30*V(I))-10
690 IF S0=0 THEN 740
700 F1=F(I,J)-F1-U9
710 IF F1>0 THEN 760
720 Y=0
730 GO TO 850
740 F1=F(I,J)
750 Y=4.5*S*F1
760 IF L0=0 THEN 780
770 Y=6*LGT(F1)+21
780 IF D7=1 THEN 840
790 MOVE X,Y
800 RMOVE -0.13,-0.45
```

```
810 IF Y<0 THEN 870
820 PRINT "+"
830 GO TO 870
840 IF I>1 THEN 860
850 MOVE X,Y
860 DRAW X,Y
870 NEXT I
880 S0=0
890 IF L0<>1 THEN 1390
900 IF D6=0 THEN 1390
910 FOR I=1 TO 24
920 R2=I=11
930 R3=I>11
940 R1=1+R2+2*R3
950 MOVE 30*V(I),6*LGT(0.0069396166/R1)+21
960 RMOVE -0.13,-0.45
970 PRINT "-"
980 NEXT I
990 GO TO 1390
1000 RETURN
1010 PRINT "__  RETRIEVE DATA FROM FILE # ";
1020 J=1
1030 INPUT N0
1040 FIND N0
1050 PRINT " _START WITH SPECTRUM DAY HOUR: ";
1060 INPUT M0,M1
1070 PRINT " _LAST SPECTRUM AT DAY HOUR: ";
1080 INPUT O1,O2
1090 INPUT @33:L9,L7
1100 L9=L9+1900
1110 INPUT @33:L1(J),L2(J)
1120 IF L1(J)<M0 THEN 1150
1130 IF L2(J)<M1 THEN 1150
1140 GO TO 1260
1150 FOR I=1 TO 33
1160 INPUT @33:K7
1170 NEXT I
1180 GO TO 1110
1190 INPUT @33:L1(J),L2(J)
1200 INPUT @33:K7
1210 FOR I=1 TO 24
1220 INPUT @33:K7
1230 R2=I=11
1240 R3=I>11
1250 R1=1+R2+2*R3
1260 F(I,J)=68.8612*0.964599↑K7/R1
1270 NEXT I
1280 FOR I=1 TO 8
1290 INPUT @33:K7
1300 NEXT I
1310 J=J+1
1320 IF J>16 THEN 1350
1330 IF L1(J-1)<O1 THEN 1190
1340 IF L2(J-1)<O2 THEN 1190
1350 N7=J-1
1360 Q$=CHR(65+L7)
1370 PRINT "_  DATA RETRIEVED GFROM FILE # ";N0
1380 RETURN
1390 HOME
1400 PRINT "__",L9
1410 PRINT " Solrad 11";Q$
1420 PRINT L1(J);L2(J)
1430 PRINT " INDEX = ";J
1440 IF L0=0 THEN 1490
1450 IF L0=1 THEN 1480
1460 PRINT "_ Log-log plot"
1470 GO TO 1490
1480 PRINT "_ Semi-log Plot"
1490 IF S=1 THEN 1510
1500 PRINT " scale = ";S
```

```
1510 HOME
1520 L0=1
1530 RETURN
1540 PAGE
1550 L=-1
1560 K=1
1570 FOR X0=0 TO 99 STEP 33
1580 FOR Y0=0 TO 75 STEP 25
1590 VIEWPORT X0,X0+30,75-Y0,95-Y0
1600 L=L+1
1610 IF L>0 THEN 1720
1620 PRINT "__  Solrad 11";Q$
1630 PRINT "_       ";L9
1640 PRINT "_       ";L1(1)
1650 IF L0=0 THEN 1680
1660 PRINT "_  Semi-log plot"
1670 GO TO 2080
1680 IF S=1 THEN 2080
1690 PRINT " scale = ";
1700 PRINT S
1710 GO TO 2080
1720 IF L>N7 THEN 2080
1730 IF L0=0 THEN 1760
1740 AXIS 2.137,6
1750 GO TO 1770
1760 AXIS 2.137,0
1770 MOVE 15,25
1780 PRINT L2(L)
1790 H1=1
1800 FOR I=1 TO 24
1810 IF L0=2 THEN 1840
1820 X=30*V(I)
1830 GO TO 1850
1840 X=20*LGT(30*V(I))-10
1850 F1=F(I,L)
1860 Y=4.5*S*F1
1870 IF L0=0 THEN 1890
1880 Y=6*LGT(F1)+21
1890 IF D7=1 THEN 1940
1900 IF Y<0 THEN 1970
1910 MOVE X,Y
1920 RDRAW 0,0
1930 GO TO 1970
1940 IF I>1 THEN 1960
1950 MOVE X,Y
1960 DRAW X,Y
1970 NEXT I
1980 K=K+1
1990 IF L0<>1 THEN 2080
2000 IF D8=0 THEN 2080
2010 FOR I=1 TO 24
2020 R2=I=11
2030 R3=I>11
2040 R1=1+R2+2*R3
2050 MOVE 30*V(I),6*LGT(0.0069396166/R1)+21
2060 RDRAW 0,0
2070 NEXT I
2080 NEXT Y0
2090 NEXT X0
2100 HOME
2110 PRINT "G";
2120 RETURN
2130 INPUT Z8
2140 W2=(1403.7*V(Z8)-B)↑2/A↑2
2150 F1=((1+1/C)/(1+W2/C))↑C*10↑D
2160 U9=F(Z8,J)-F1
2170 C=K8(J)
2180 B=V7(J)
2190 A=W0(J)
2200 D=H8(J,K0)
```

```
2210 H=N1(J)
2220 L=8
2230 U1=(B-3.1*A)/46.794
2240 U2=(B+3.1*A)/46.794
2250 IF K0=1 THEN 2310
2260 U1=U1
2270 U2=U2
2280 IF U1>5 THEN 2310
2290 U1=5
2300 U2=20
2310 FOR X=U1 TO U2 STEP 0.2
2320 W2=(46.794*X-B)↑2/A↑2
2330 IF K0=2 THEN 2360
2340 F1=H*EXP(-W2)*10↑D
2350 GO TO 2120
2360 F1=((1+1/C)/(1+W2/C))↑C*10↑D
2370 IF L0=1 THEN 2400
2380 Y=4.5*S*F1
2390 GO TO 2410
2400 Y=6*LGT(F1)+21
2410 IF L<=9 THEN 2440
2420 DRAW X,Y
2430 GO TO 2450
2440 MOVE X,Y
2450 L=F1
2460 NEXT X
2470 PRINT "↑JJJJJJJJJJJJ"
2480 IF K0=2 THEN 2510
2490 PRINT "Maxwellian fit"
2500 GO TO 2520
2510 PRINT "Kappa dist fit"
2520 PRINT "_Bulk Vz = ";V7(J)
2530 PRINT "Therm w. = ";A
2540 PRINT "Den = ";N1(J);"/cc"
2550 IF K0=1 THEN 2570
2560 PRINT "Kappa = ";C
2570 RETURN
```

APPENDIX C

LISTING OF THREE DIMENSIONAL PLOT PROGRAM

```
1 GO TO 200
2 RETURN
4 L0=0
5 GO TO 390
8 PRINT "NEW ALPHA EQUALS ";
10 INPUT A
11 GO TO 390
12 PRINT "NEW BETA EQUALS ";
14 INPUT B
15 GO TO 390
16 PRINT "_ LIST DATA FROM FILE # ";
17 INPUT N0
18 FIND N0
19 GO TO 85
20 PAGE
21 LIST
22 RETURN
23 GO TO 390
24 IF H0=0 THEN 1240
25 GO TO 1270
32 GO TO 100
36 L0=0
37 GO TO 41
40 L0=1
41 PRINT "INPUT SPECTRUM INDEX: ";
42 INPUT J
43 GO TO 1190
44 L0=1
45 GO TO 390
48 PRINT "O(X,Y) = "
49 INPUT X9,Y9
51 GO TO 390
52 PRINT "SCALE EQUALS ";
53 INPUT S
54 GO TO 390
56 GO TO 1600
60 GO TO 1370
64 H0=1
65 GO TO 360
72 GO TO 100
76 GO TO 360
80 C0=1
81 GO TO 410
85 INPUT @33:M8,M9,M,M6,M7
86 PAGE                                                                 ";M8;M9
87 PRINT M;"
88 PRINT M6
89 PRINT M7
90 FOR I=1 TO 24
91 INPUT @33:M
92 PRINT "      ",M
93 NEXT I
94 FOR I=1 TO 11
95 INPUT @33:M
96 PRINT M
97 NEXT I
98 GO TO 90
100 PRINT "_ INPUT SPECTRUM HOUR : ";
110 INPUT M
120 J=0
130 J=J+1
140 IF L2(J)=M THEN 180
150 IF J<N7 THEN 130
160 PRINT "_ SPECTRUM NOT FOUND"
170 RETURN
180 L0=0
190 GO TO 1190
200 DIM F(24,20)
210 DIM C$(2),A$(1),B$(1)
```

```
220 DIM V(24),T1(30),L1(30),L2(30)
230 H0=1
240 N7=0
250 DELETE 1,1
260 FOR K=1 TO 24
270 READ V(K)
280 NEXT K
290 DATA 0.167,0.189,0.209,0.227,0.243,0.259,0.273,0.287
300 DATA 0.3,0.313,0.33,0.359,0.39,0.419,0.447,0.473
310 DATA 0.497,0.52,0.543,0.565,0.586,0.606,0.626,0.645
320 READ A,B,S,T2,E1,E2,X9,Y9
330 DATA 30,45,2,0,2,2,0,0
340 PAGE
350 SET DEGREES
360 PAGE
370 PRINT "G READY _  PROGRAM DOES NOT INCLUDE_   KEYBOARD DN INPUT__G";
380 RETURN
390 PAGE
400 C0=0
410 WINDOW -12.5-X9,52.5-X9,-20-Y9,30-Y9
420 VIEWPORT 0,130,0,100
430 H0=0
440 H1=0
450 X0=20*S*COS(B)
460 Y0=20*S*SIN(B)*SIN(A)
470 Y1=12*S*COS(A)
480 X2=20*S*SIN(B)
490 Y2=-20*S*COS(B)*SIN(A)
500 MOVE 0,0
510 DRAW X0,Y0
520 PRINT " t"
530 MOVE 0,0
540 DRAW 0,Y1
550 IF L0=1 THEN 580
560 PRINT " f"
570 GO TO 590
580 PRINT " log f"
590 MOVE 0,0
600 DRAW X2,Y2
610 PRINT " v"
620 FOR K=1 TO 24 STEP 23
630 X3=X2*V(K)
640 Y3=Y2*V(K)
650 MOVE X3,Y3
660 RDRAW X0,Y0
670 NEXT K
680 IF C0=1 THEN 930
690 T2=0
700 T1(N7)=0
710 FOR J=1 TO N7
720 IF J=1 THEN 760
730 T2=T2+T1(J-1)
740 T=J+T2-1
750 GO TO 770
760 T=0
770 FOR I=1 TO 24
780 V1=20*V(I)
790 D=SQR(V1↑2+T↑2)
800 C=B+ATN(T/V1)
810 X=S*D*SIN(C)
820 IF L0=0 THEN 860
830 Y8=3*LGT(F(I,J))+8
840 Y=-S*D*COS(C)*SIN(A)+S*COS(A)*Y8
850 GO TO 870
860 Y=-S*D*COS(C)*SIN(A)+S*COS(A)*F(I,J)
870 IF I>1 THEN 890
880 MOVE X,Y
890 DRAW X,Y
900 NEXT I
910 NEXT J
```

```
920 GO TO 2050
930 FOR I=1 TO 24
940 V1=20*V(I)
950 V2=V1↑2
960 T3=0
970 T1(N7)=0
980 Y8=-1
990 FOR J=1 TO N7
1000 IF J=1 THEN 1040
1010 T3=T3+T1(J-1)
1020 T=J+T3-1
1030 GO TO 1050
1040 T=0
1050 D=SQR(V2+T↑2)
1060 C=B+ATN(T/V1)
1070 X=S*D*SIN(C)
1080 IF L0=0 THEN 1120
1090 Y8=3*LGT(F(I,J))+8
1100 Y=-S*D*COS(C)*SIN(A)+S*COS(A)*Y8
1110 GO TO 1130
1120 Y=-S*D*COS(C)*SIN(A)+S*COS(A)*F(I,J)
1130 IF J>1 THEN 1150
1140 MOVE X,Y
1150 DRAW X,Y
1160 NEXT J
1170 NEXT I
1180 GO TO 2050
1190 WINDOW 0,25,0,30
1200 VIEWPORT 30,130,20,100
1210 PAGE
1220 AXIS
1230 H1=1
1240 FOR I=1 TO 24
1250 X=20*V(I)
1260 IF L0=0 THEN 1290
1270 Y=S*E1*(LOG(F(I,J))+E2)
1280 GO TO 1300
1290 Y=S*F(I,J)
1300 IF I>1 THEN 1320
1310 MOVE X,Y
1320 DRAW X,Y
1330 NEXT I
1340 HOME
1350 GO TO 2050
1360 RETURN
1370 K7=0
1380 PRINT "_ STORE DATA ON FILE # ";
1390 INPUT N0
1400 FIND N0
1410 PRINT @33:L9
1420 PRINT @33:L7
1430 FOR K=1 TO N7
1440 PRINT @33:L1(K)
1450 PRINT @33:L2(K)
1460 PRINT @33:K7
1470 FOR I=1 TO 24
1480 R2=I=11
1490 R3=I>11
1500 R1=1+R2+2*R3
1510 K0=117.09429-27.744786*LOG(R1*F(I,K))
1520 PRINT @33:K0
1530 NEXT I
1540 FOR M=1 TO 8
1550 PRINT @33:K7
1560 NEXT M
1570 NEXT K
1580 PRINT "DATA STORED IN FILE # ";N0
1590 RETURN
1600 PRINT "__  RETRIEVE DATA FROM FILE # ";
1610 J=1
```

```
1620 INPUT N0
1630 FIND N0
1640 PRINT " _START WITH SPECTRUM DAY HOUR: ";
1650 INPUT M0,M1
1660 PRINT " _LAST SPECTRUM AT DAY HOUR: ";
1670 INPUT O1,O2
1680 INPUT @33:L9,L7
1690 L9=L9+1900
1700 INPUT @33:L1(J),L2(J)
1710 IF L1(J)<M0 THEN 1750
1720 IF L2(J)<M1 THEN 1750
1730 L8=L2(J)
1740 GO TO 1790
1750 FOR I=1 TO 33
1760 INPUT @33:K7
1770 NEXT I
1780 INPUT @33:L1(J),L2(J)
1790 INPUT @33:K7
1800 FOR I=1 TO 24
1810 INPUT @33:K7
1820 R2=I=11
1830 R3=I>11
1840 R1=1+R2+2*R3
1850 F(I,J)=68.0612*0.964599↑K7/R1
1860 NEXT I
1870 FOR I=1 TO 8
1880 INPUT @33:K7
1890 NEXT I
1900 IF J=1 THEN 1990
1910 L6=L8
1920 L8=L2(J)
1930 L3=L8-L6
1940 IF L3>0 THEN 1960
1950 L3=L3+2400
1960 IF L3<40 THEN 1980
1970 L3=L3-40
1980 T1(J-1)=L3/2-1
1990 J=J+1
2000 IF L1(J-1)<O1 THEN 1780
2010 IF L2(J-1)<O2 THEN 1780
2020 N7=J-1
2030 PRINT "_  DATA RETRIEVED GFROM FILE # ";N0
2040 RETURN
2050 HOME
2060 PRINT "_ _",L9
2070 IF L7=1 THEN 2100
2080 PRINT " Solrad 11A"
2090 GO TO 2110
2100 PRINT " Solrad 11B"
2110 IF H1=1 THEN 2150
2120 PRINT L1(1);L2(1)
2130 PRINT L1(N7);L2(N7)
2140 GO TO 2190
2150 PRINT L1(J);L2(J)
2160 PRINT " INDEX = ";J
2170 IF L0=0 THEN 2190
2180 PRINT "_ Semi-log plot"
2190 HOME
2200 RETURN
```

REFERENCES

Vasyliunas, Vytenis M., "Deep Space Plasma Measurement", Methods of Experimental Physics, V. 98, 1971, Academic Press Inc., New York

Gorin, Joseph M., Instrumentation of a Plasma Probe Space Experiment, M.I.T. Master's Thesis, Dept. of Electrical Engineering, January 1974.